



COMILLAS
UNIVERSIDAD PONTIFICIA

ICAI

GRADO EN INGENIERÍA EN TECNOLOGÍAS
INDUSTRIALES

TRABAJO FIN DE GRADO

**OFFLINE OPTIMAL POWER FLOW AND DATA
DRIVEN CONTROL FOR THE REDUCTION OF
THE CARBON FOOTPRINT OF A DISTRIBUTION
NETWORK**

Autor: Álvaro Esteban Otero

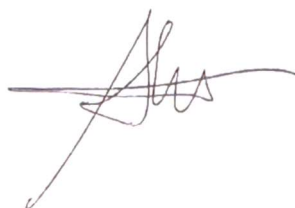
Director: Ian Hiskens

Madrid

Julio de 2020

Declaro, bajo mi responsabilidad, que el Proyecto presentado con el título:
“Offline Optimal Power Flow and Data Driven Control for the Reduction of the Carbon Footprint of a Distribution Network”

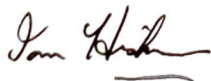
en la ETS de Ingeniería - ICAI de la Universidad Pontificia Comillas en el curso académico 2019/2020 es de mi autoría, original e inédito y no ha sido presentado con anterioridad a otros efectos. El Proyecto no es plagio de otro, ni total ni parcialmente y la información que ha sido tomada de otros documentos está debidamente referenciada.



Fdo.: Álvaro Esteban Otero

Fecha: 16/07/2020

Autorizada la entrega del proyecto
EL DIRECTOR DEL PROYECTO



Fdo.: Ian Hiskens

Fecha: 16/07/2020



COMILLAS
UNIVERSIDAD PONTIFICIA

ICAI

GRADO EN INGENIERÍA EN TECNOLOGÍAS
INDUSTRIALES

TRABAJO FIN DE GRADO

**OFFLINE OPTIMAL POWER FLOW AND DATA
DRIVEN CONTROL FOR THE REDUCTION OF
THE CARBON FOOTPRINT OF A DISTRIBUTION
NETWORK**

Autor: Álvaro Esteban Otero

Director: Ian Hiskens

Madrid

Julio de 2020

FLUJO DE CARGA ÓPTIMO Y CONTROL BASADO EN DATOS PARA LA REDUCCIÓN DE LA HUELLA DE CARBONO DE UNA RED DE DISTRIBUCIÓN

Autor: Esteban Otero, Álvaro

Director: Hiskens, Ian

Entidad Colaboradora: University of Michigan, Ann Arbor

RESUMEN DEL PROYECTO

1. Introducción

Los avances tecnológicos pueden llegar a ser una moneda de dos caras. Por un lado, ofrecen nuevas posibilidades para continuar avanzando como sociedad. Sin embargo, pueden venir acompañados de desafíos que complican su implementación cuestionando la sostenibilidad del nuevo paradigma. Este es el caso de la red eléctrica. Las fuentes renovables están consideradas como el futuro del suministro de energía de la sociedad. Se espera que puedan sustituir a las fuentes convencionales de energía y logren eliminar la huella de carbono de la energía que se consume. No obstante, estas tecnologías suponen también un desafío para la fiabilidad del sistema, ya que introducen una variabilidad añadida que complica aún más la tarea de operar y controlar la red. Dicha tarea está formada por dos deberes diferentes: por un lado, el control de la tensión; por otro, el control de la frecuencia. Poniendo el foco sobre la primera de las anteriores tareas, hasta ahora el control de tensión se había realizado a través de tres estrategias principales: el control de la corriente de excitación en las centrales de generación, la modificación de las tomas de los transformadores y la conexión de elementos de derivación. El proceso de toma de decisiones se toma de manera centralizada, mediante la observación de los valores de todas las variables de la red. A parte del coste de la infraestructura de comunicaciones necesaria, esta aproximación centralizada de control tiene dificultades para aprovechar la flexibilidad que aportan los recursos de generación distribuida. Este aspecto podría ser mejorado mediante el desarrollo de controles locales, que aprovechen las medidas disponibles en un nudo para calcular la generación óptima. La combinación

de estrategias centralizadas y locales será esencial en el futuro para proporcionar un control distribuido que facilite el camino hacia la sostenibilidad.

2. Metodología

Este estudio contiene dos partes diferenciadas: en primer lugar, el desarrollo de un flujo de carga óptimo centralizado; en segundo, el diseño y test de controles locales.

La primera fase del proyecto trata de proponer un modelo que minimice la huella de carbono de una red de distribución a lo largo de un período de operación de tres días. Mediante la carga y descarga óptima de las baterías presentes en la red, se logra reducir las emisiones de CO₂ cargando las baterías durante períodos de baja intensidad y descargándolas en los períodos de alta intensidad de carbono. Los datos aportados al modelo son las curvas de demanda, la curva de radiación solar y la curva de la intensidad de carbono de la red principal. Por su parte, el modelo proporciona una base de datos con los puntos de operación óptimos, que será empleada para el diseño de los controles locales. El flujo de carga óptimo que se propone en este estudio se apoya en el flujo de carga DistFlow, y presenta la siguiente estructura:

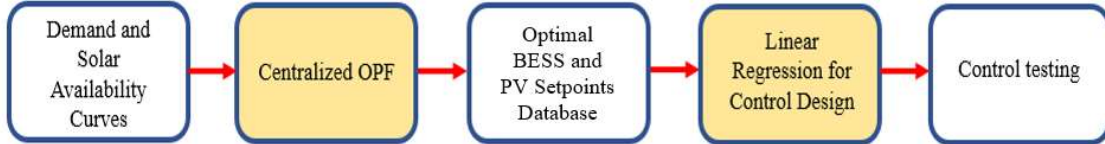
$$\min \sum_{t=1}^{T_{hor}} \left\{ \sum_{n=1}^N (Eg_t * Pg_{n,t}) \right\} * \Delta t$$

s.t.:

$$\begin{aligned} l_{j,t} &= |I_{j,t}|^2 \\ v_{n,t} &= |V_{n,t}|^2 \\ v_{n,t} &= v\pi_{n,t} - 2r_n P_{j,t} - 2x_n Q_{j,t} + (r_n^2 + x_n^2) * l_{j,t} \\ \frac{P_{j,t}^2 + Q_{j,t}^2}{v\pi_{n,t}} &= l_{j,t} \\ \sum_{k:n \rightarrow k} P_{k,t} &= p_{n,t} + P_{j,t} - r_n l_{j,t} \\ \sum_{k:n \rightarrow k} Q_{k,t} &= q_{n,t} + Q_{j,t} - x_n l_{j,t} \\ p_{n,t} &= Pg_{n,t} - Pd_{n,t} \\ q_{n,t} &= Qg_{n,t} - Qd_{n,t} \\ Pg_c^{min} &\leq Pg_{c,t} \leq Pg_c^{max} \\ Qg_c^{min} &\leq Qg_{c,t} \leq Qg_c^{max} \end{aligned}$$

$$\begin{aligned}
0 &\leq P_{g,r,t} \leq Avail(t) * Surfcoef_r * P_{g_r}^{max} \\
0 &\leq l_{j,t} \leq l_j^{max} \\
v_n^{min} &\leq v_{n,t} \leq v_n^{max} \\
p_{b,t} &= P_{g_{b,t}} - P_{d_{b,t}} + x_{dis_{b,t}} * P_{dis_{b,t}} - x_{ch_{b,t}} * P_{ch_{b,t}} \\
0 &\leq P_{ch_{b,t}} \leq P_{ch_b}^{max} \\
0 &\leq P_{dis_{b,t}} \leq P_{dis_b}^{max} \\
x_{ch_{b,t}} + x_{dis_{b,t}} &\leq 1 \\
E_{bat_{b,1}} &= E_{initial} \\
E_{bat_{b,t}} &= E_{bat_{b,t-1}} + \left(x_{ch_{b,t}} * \eta * P_{ch_{b,t}} - x_{dis_{b,t}} * \frac{P_{dis_{b,t}}}{\eta} \right) * \Delta t \\
(1 - DoD) * E_{bat_{cap}} &\leq E_{bat_{b,t}} \leq PU_{limit} * E_{bat_{cap}} \\
E_{bat_{b,end}} &= E_{initial}
\end{aligned}$$

La base de datos obtenida en el paso anterior sirve como set de entrenamiento para los controles locales. Después de procesar los datos mediante técnicas de regresión, se diseñan los controles. A continuación, se valora el desempeño de dichos controles mediante una comparación de su respuesta con la proporcionada por el flujo de carga, que es considerada como absolutamente óptima.

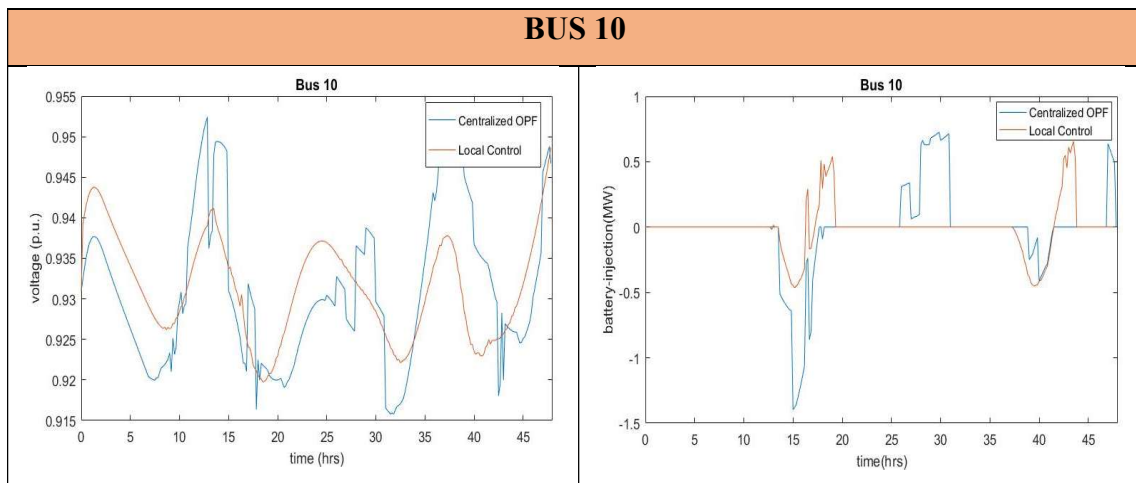


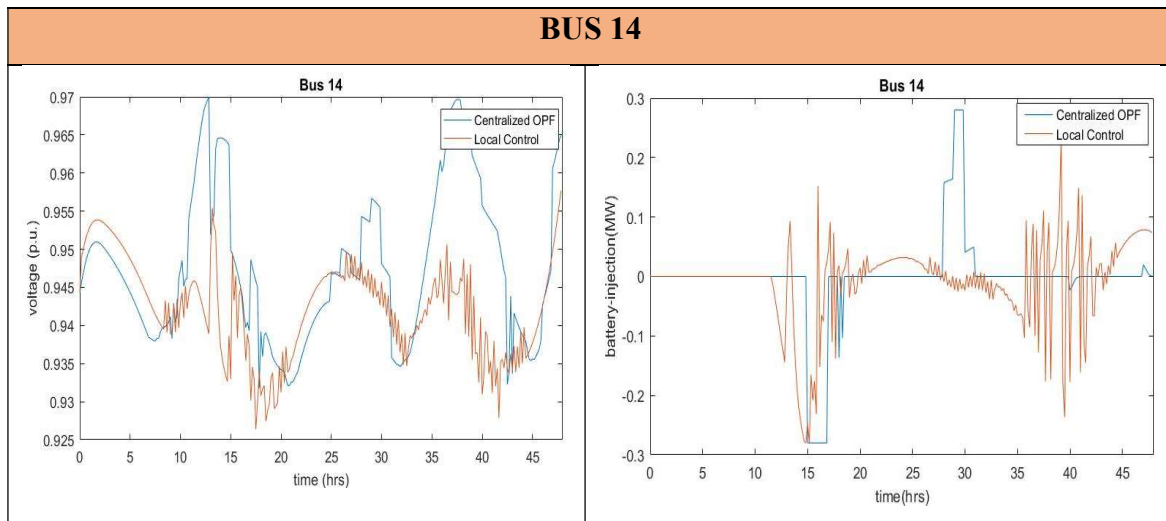
3. Resultados

La metodología presentada ha sido implementada para dos casos diferentes: una red de 4 nodos y otra red de 18 nodos. Los resultados obtenidos durante la primera etapa para el caso de 4 nodos impidieron la continuación con el diseño de los controles. El rango de tensiones obtenido tras la ejecución del flujo de carga no era suficientemente amplio como para desarrollar un modelo robusto. Sin embargo, merece la pena comparar la reducción de emisiones obtenida mediante el flujo de carga para cada uno de los casos:

CASE	Emissions without BESS in 3-day period (kg CO ₂ e)	Emissions with BESS in 3-day period (kg CO ₂ e)	Annual reduction of emissions (kg CO ₂ e)	N° of batteries installed	Total annual cost of the batteries (\$)	Marginal cost of the carbon footprint reduction (\$/kg CO ₂ e)
4-Bus	7,885	7,816	8,395	80	60,000	7.15
18-Bus	74,578	72,613	239,075	1040	780,000	3.26

El flujo de carga se ejecutó para cada uno de los casos con y sin baterías. De la tabla que se presenta encima, se puede deducir que la introducción de las baterías produce una reducción de la huella de carbono para ambos casos. No obstante, el coste marginal de dicha reducción es un 50% inferior para el caso de 18 nodos, lo que sugiere que hay potencial de escala.





Las gráficas que se presentan encima incluyen la respuesta de los controles diseñados para el caso de 18 nodos. Los dos nodos son representativos de las respuestas obtenidas, que se dividen en dos grupos: en primer lugar, el grupo representado por el nodo 10, que muestra una respuesta más amortiguada; en segundo, el grupo representado por el nodo 14, que muestra variaciones continuas en la inyección de la batería que se traducen en variaciones en tensión. Estos resultados pretenden ser el punto de partida de trabajos futuros que se centren en la investigación y desarrollo de nuevos modelos para los controles locales.

4. Conclusiones

A partir de los resultados obtenidos, se pueden extraer varias conclusiones. Con respecto al entrenamiento y prueba de los controles, es necesario ampliar la base datos mediante la simulación de más estados posibles de la red, de manera que el modelo obtenido podrá ser más fiable. Además, otros modelos de regresión pueden ser estudiados para proporcionar una mejor respuesta de los controles.

En cuanto a la contribución realizada por el flujo de carga óptimo, merece la pena analizar la reducción de emisiones obtenida. Siendo las emisiones de CO₂ uno de los principales desafíos para la sostenibilidad, es esencial promover nuevas estrategias que ayuden a reducirlas. Esta necesidad se puede apreciar en el compromiso asumido por los miembros

de las Naciones Unidas a través de la firma de los Objetivos de Desarrollo Sostenible. Este proyecto trata de proponer una metodología que pueda ayudar a atajar uno de los ODSs: “Garantizar el acceso para todos a energía asequible, segura, sostenible y moderna”, centrándose principalmente en el objetivo de “Para 2030 incrementar sustancialmente el porcentaje de energía renovable en mix de energía global”. Mediante el aprovechamiento de la flexibilidad proporcionada por las baterías, el flujo de carga óptimo propuesto es capaz de incrementar la energía renovable consumida en la red. De esta manera, este estudio también ataja el problema de la sostenibilidad desde un punto de vista del consumo, que se resume en el ODS 12: “Garantizar patrones de consumo y de producción sostenible” con el objetivo de “Para 2030, lograr una gestión sostenible y un uso eficiente de los recursos naturales”. De este modo, la metodología propuesta proporciona una base de conocimiento sobre cómo se puede gestionar el mix de energía actual de una manera más eficiente para mejorar su desempeño medioambiental.

OFFLINE OPTIMAL POWER FLOW AND DATA DRIVEN CONTROL FOR THE REDUCTION OF THE CARBON FOOTPRINT OF A DISTRIBUTION NETWORK

Author: Esteban Otero, Álvaro

Director: Hiskens, Ian

Collaborating Organization: University of Michigan, Ann Arbor

PROJECT SUMMARY

1. Introduction

Technological developments can be a two-face coin. On the one hand, they offer new possibilities in order to keep evolving as a society. However, technological innovations come as well with challenges that complicate their implementation by questioning the sustainability of the new paradigm. This is the case of the electrical grid. Renewable energy sources are considered to be the future of society's power supply by, eventually, eliminating the carbon footprint of the energy consumed. Nevertheless, these technologies pose a threat to the system's reliability since their variability further complicates the task of operating and controlling the grid. The task of operating the grid is divided in two different subtasks: voltage control and frequency control. Focusing on the voltage control, so far this task has been performed by implementing three principal strategies: shunt devices, tap-changing transformers and excitation control at generating stations. The process of decision is carried out in a centralized way, that is from the ability of knowing the values of all the variables in the grid. Beyond the cost of the communication infrastructure needed, this centralized approach seems to struggle to harness the flexibility provided by DERs, which could be enhanced by the implementation of local controls. The combination of centralized and local control will be key in the future of the power grid by providing a distributed approach which could ease the path towards sustainability.

The aim of this study is to propose a methodology that combines centralized and local strategies in order to reduce the carbon footprint of a distribution network. First, the

development of a centralized OPF serves as benchmark for the optimal dispatch of the grid. This optimal dispatch condensed in a database of optimal setpoint, which underpins the design of local controls. The combination of these two stages of the study aims to provide local voltage controls that guarantee safe voltage values while ensuring an optimal operation of both the generation panels and the energy storage systems. The coordination of these two elements will be key for the sustainable future of distribution networks.

2. Methodology

The study consists of two different parts: first, the development of the offline centralized OPF; second, the design and testing of the data-driven local controls.

The first stage of the project, the development of the centralized OPF, aims to provide a model that minimizes the carbon footprint of a distribution grid throughout a 3-day operation period. By optimally charging and discharging the BESS installed in the grid, the model is able to reduce the CO₂ emissions by charging the batteries during low intensity periods and discharging them during high intensity periods. The inputs to the model are the demand curves, the solar availability curve and the grid's carbon intensity curve; the output is a database of optimal setpoint that underpins the next step of the study: the design of the local voltage controls. The proposed OPF is underpinned by the DistFlow power flow, and looks as follows:

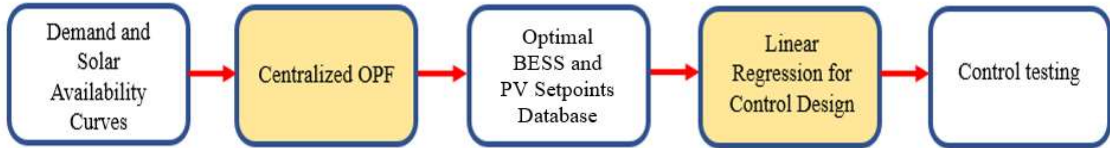
$$\min \sum_{t=1}^{T_{hor}} \left\{ \sum_{n=1}^N (Eg_t * Pg_{n,t}) \right\} * \Delta t$$

s.t.:

$$\begin{aligned} l_{j,t} &= |I_{j,t}|^2 \\ v_{n,t} &= |V_{n,t}|^2 \\ v_{n,t} &= v\pi_{n,t} - 2r_n P_{j,t} - 2x_n Q_{j,t} + (r_n^2 + x_n^2) * l_{j,t} \\ \frac{P_{j,t}^2 + Q_{j,t}^2}{v\pi_{n,t}} &= l_{j,t} \\ \sum_{k:n \rightarrow k} P_{k,t} &= p_{n,t} + P_{j,t} - r_n l_{j,t} \\ \sum_{k:n \rightarrow k} Q_{k,t} &= q_{n,t} + Q_{j,t} - x_n l_{j,t} \\ p_{n,t} &= Pg_{n,t} - Pd_{n,t} \end{aligned}$$

$$\begin{aligned}
q_{n,t} &= Qg_{n,t} - Qd_{n,t} \\
Pg_c^{min} &\leq Pg_{c,t} \leq Pg_c^{max} \\
Qg_c^{min} &\leq Qg_{c,t} \leq Qg_c^{max} \\
0 &\leq Pg_{r,t} \leq Avail(t) * Surfcoef_r * Pg_r^{max} \\
0 &\leq l_{j,t} \leq l_j^{max} \\
v_n^{min} &\leq v_{n,t} \leq v_n^{max} \\
p_{b,t} &= Pg_{b,t} - Pd_{b,t} + xdis_{b,t} * Pdis_{b,t} - xch_{b,t} * Pch_{b,t} \\
0 &\leq Pch_{b,t} \leq Pch_b^{max} \\
0 &\leq Pdis_{b,t} \leq Pdis_b^{max} \\
xch_{b,t} + xdis_{b,t} &\leq 1 \\
Ebat_{b,1} &= Einitial \\
Ebat_{b,t} &= Ebat_{b,t-1} + \left(xch_{b,t} * \eta * Pch_{b,t} - xdis_{b,t} * \frac{Pdis_{b,t}}{\eta} \right) * \Delta t \\
(1 - DoD) * Ebat_{cap} &\leq Ebat_{b,t} \leq PU_{limit} * Ebat_{cap} \\
Ebat_{b,end} &= Einitial
\end{aligned}$$

The database obtained in the previous stage serves as training set for the local controls. After processing the data by means of regression techniques, local controls are designed. The performance of these controls is then assessed by comparing its response to the optimal benchmark set by the OPF.

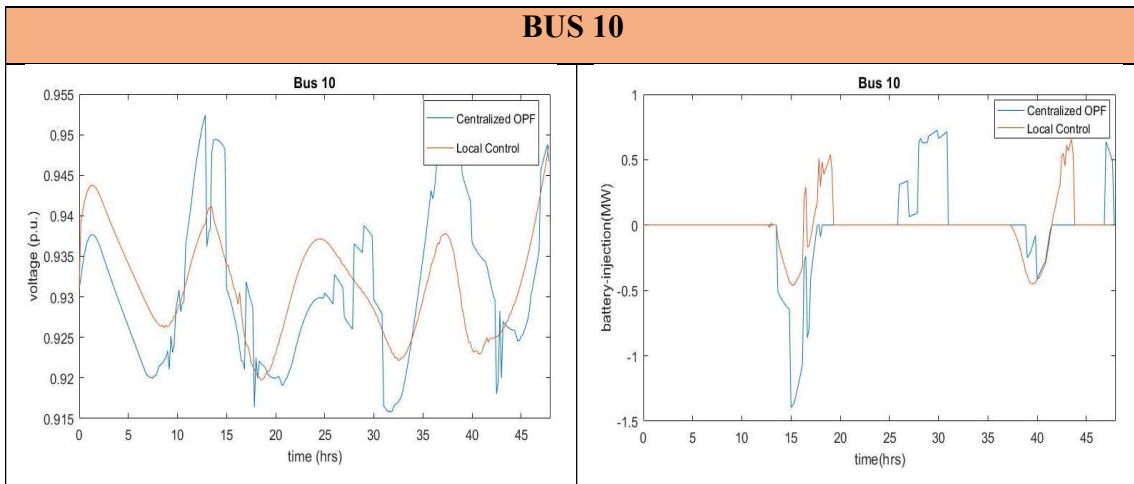


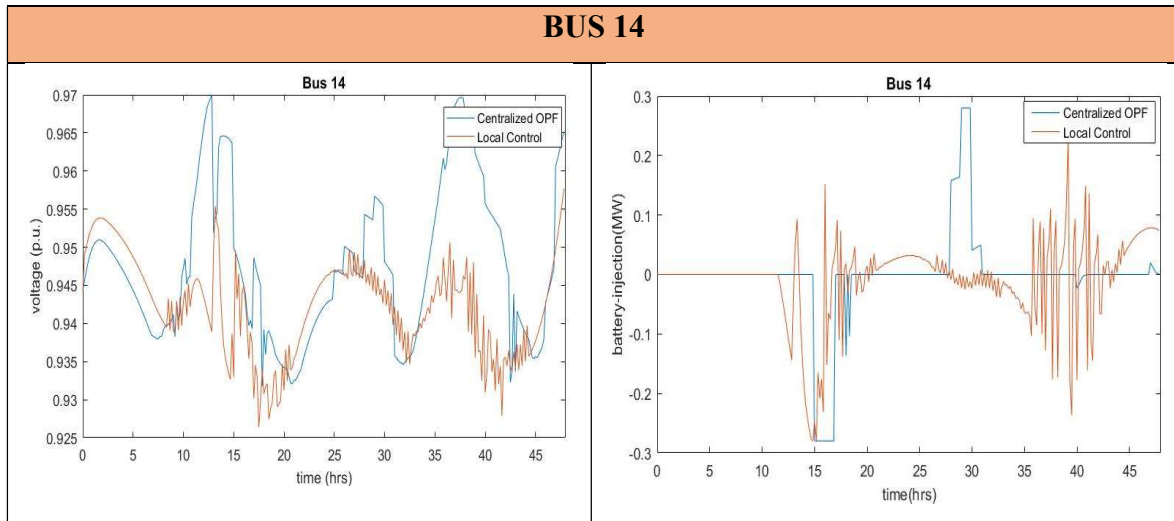
3. Results

The above presented methodology was tested for two different cases: a 4-bus grid and an 18-bus grid. The results yielded by the 4-bus case during the first stage impede the continuation to the next stage, since the range of the voltages obtained was not large enough to develop a robust model. However, it is worth analyzing the differences in the performance of the OPF for the two cases:

CASE	Emissions without BESS in 3-day period (kg CO ₂ e)	Emissions with BESS in 3-day period (kg CO ₂ e)	Annual reduction of emissions (kg CO ₂ e)	N° of batteries installed	Total annual cost of the batteries (\$)	Marginal cost of the carbon footprint reduction (\$/kg CO ₂ e)
4-Bus	7,885	7,816	8,395	80	60,000	7.15
18-Bus	74,578	72,613	239,075	1040	780,000	3.26

The OPF was run for the cases with and without BESS. From the table above presented, it can be inferred that the introduction of the batteries yielded a reduction of the carbon footprint for both cases. However, the marginal monetary cost of this enhancement was 50% lower for the 18-bus case than the 4-bus case, which suggests there is potential for scalability.





The graphs above presented include the response of the controls designed for the 18-bus case. These two buses are representative of the characteristics of the responses obtained, which are divided into two groups: first, the group of responses represented by bus 10, which yields a softer voltage response; second, the group represented by bus 14, which shows continuous fluctuations in the injection of the battery which translate into fluctuations in the voltage. This results could be the starting point of future work, which focuses on the research and design of new models for the local voltage controls.

4. Conclusions

From the results obtained several conclusions can be drawn. Regarding the training and testing of the control, it is necessary to produce a larger training set so that the model obtained can be more robust. Moreover, other regression models could be researched in order to enhance the response of the controls.

Regarding the contribution made by the OPF, it is worth analyzing the reduction of the carbon footprint achieved. Being CO₂ emissions one of the main challenges towards sustainability, it is key to produce new strategies that help to reduce them. This is exemplified by the commitment signed by the members of the United Nations through the Sustainable Development Goals. This study tries to propose a methodology that helps tackle one of the SDGs: “Ensure access to affordable, reliable, sustainable and modern

energy for all”, focusing on the target “By 2030, increase substantially the share of renewable energy in the global energy mix” as the primary goal. By harnessing the flexibility provided by the BESS, the proposed OPF is able to increase the consumed renewable power in the grid. Therefore, this research addresses sustainability from a consumption point of view, which is summarized in the 12th SDG: “Ensure sustainable consumption and production patterns” with the goal of “By 2030, achieve sustainable management and efficient use of natural resources”. Thus, the proposed methodology provides insight on how the current energy mix could be managed in a more efficient way to enhance its environmental performance.

TABLE OF CONTENTS

1. Introduction.	1
1.1. Motivation and Background.	1
1.1.1. Paris Agreement and Its Implications.	1
1.1.2. Challenges of the Implementation of Renewables.	3
1.2. Objective.	6
1.3. Overview.	6
2. State of the Art.	7
2.1. Voltage Control Today.	7
2.2. Centralized, Decentralized and Distributed Control	9
2.3. The Future of Grid Operation.	10
3. Model Description.	13
3.1. Centralized Optimal Power Flow.	13
3.1.1. Multiperiod characteristics.	13
3.1.2. Objective function.	13
3.1.3. Decision variables.	14
3.1.4. DistFlow Model.	14
3.1.5. Energy sources generation limits.	16
3.1.6. Branch currents and bus voltages limitations.	17
3.1.7. Energy Storage Systems.	17
3.1.8. Complete OPF.	21
3.2. Load Curves.	22
3.2.1. Household consumption.	22
3.2.2. Industrial consumption.	23
3.2.3. Commercial consumption.	24
3.3. Solar Availability Curve.	26
3.4. Grid's Carbon Intensity Curve	27
3.5. Grid's Elements Guide.	29
3.6. Local Voltage Control.	30
3.6.1. Control Design.	30

3.6.2. Control Testing.	31
3.7. Methodology Overview.	34
4. Results Analysis.	35
4.1. Base Case: 4-bus grid.	35
4.1.1. OPF Results.	36
4.2. Case Study: 18-bus grid.	41
4.2.1. OPF Results.	42
4.2.2. Control Design.	44
4.2.3. Control Testing.	55
5. Economic and Environmental Impact Assessment.	61
6. Conclusions	63
6.1. Methodology.	63
6.2. Results.	63
6.3. Future Work and Recommendations.	64
7. References.	65
APPENDIX A: Sustainable Development Goals.	66
APPENDIX B: 4-bus Case Data.	69
APPENDIX C: 18-bus Case Data.	71
APPENDIX D: Powerwall Datasheet.	74
APPENDIX E: 4-bus Grid Centralized OPF Code.	75
APPENDIX F: 18-bus Grid Local Control Simulation Code.	81

FIGURE INDEX

Figure 1. Variation of global temperature [2].....	1
Figure 2. Global Emissions consistent with the Paris Agreement compared to current aggregated pledges [3].....	2
Figure 3. Modern Energy Mix [4]	4
Figure 4. European electricity price, November-December 2019 [5]	5
Figure 5. Structure of the study	6
Figure 6. Automatic Voltage Regulator for Generating Stations [7].....	7
Figure 7. On-Load Tap Changing Transformer [8].....	8
Figure 8. Paradigm Shift of the Power Supply Grid [9].....	9
Figure 9. Response to line congestion [10]	11
Figure 10. BESS Data-driven Local Control [6]	11
Figure 11. Comparison of performance between Centralized and Local Control [6] ...	12
Figure 12. Branch Flow Model Schematic [11]	15
Figure 13. DistFlow Schematic [11].....	15
Figure 14. Household demand.....	23
Figure 15. Daily industrial demand	24
Figure 16. Daily commercial demand	25
Figure 17. Daily variation of solar radiation	26
Figure 18. Carbon Intensity of the Spanish Grid.....	28
Figure 19. Test Commercial Load Curve	32
Figure 20. Test Residential Load Curve	32
Figure 21. Test Industrial Load Curve.....	32
Figure 22. Methodology Overview.....	34
Figure 23. 4-bus Grid schematic.....	35
Figure 24. 4-bus Grid, OPF Voltage Response	36
Figure 25. 4-bus Grid, OPF Generations	37
Figure 26. 4-bus Grid, BESS Charging and Discharging.....	38
Figure 27. 4-bus Grid, BESS Charging Source	39
Figure 28. 4-bus Grid, BESS Discharge Level.....	40

Figure 29. 18-bus Grid schematic.....	41
Figure 30. 18-bus Grid, OPF Voltage response.....	42
Figure 31. 18-bus Grid, OPF BESS energy.....	43
Figure 32. 18-bus Grid, OPF Generations.....	44

TABLE INDEX

Table 1. Day type attending to solar radiation.....	27
Table 2. Grid's Elements Guide.....	29
Table 3. Model Coefficients Analysis	50
Table 4. Model Residuals Analysis	55
Table 5. Control Response, Bus 8.....	56
Table 6. Control Response, Bus 9.....	56
Table 7. Control Response, Bus 10.....	57
Table 8. Control Response, Bus 11.....	57
Table 9. Control Response, Bus 14.....	58
Table 10. Control Response, Bus 15.....	58
Table 11. Control Response, Bus 16.....	59
Table 12. Control Response, Bus 17.....	59
Table 13. Control Response, Bus 18.....	60
Table 14. Battery unit price	61
Table 15. Economic and Environmental Evaluation	62

ABBREVIATIONS LIST

BESS: Battery Energy Storage System

CES: Conventional Energy Sources

CO₂: Carbon Dioxide

DER: Distributed Energy Sources

DG: Distributed Generation

DN: Distribution Network

GHG: Greenhouse Gas

ML: Machine Learning

OPF: Optimal Power Flow

PV: Photovoltaic

RES: Renewable Energy Sources

1. Introduction

1.1. Motivation and Background

1.1.1. Paris Agreement and Its Implications

Carbon emissions reduction is the greatest challenge society will face in the 21st century. The importance of fossil fuels in today's economic and social activity makes the task of finding alternative sources of energy a pressing and difficult issue to solve. The evidence of CO₂ effects on global warming brought the Nations together in 2016, when over 180 countries signed the Paris Agreement. With the signature of this agreement, the nations declared its commitment to keep the temperature rise of this century below 2°C compared to the pre-industrial levels [1]. The temperature increase tendency observed during the last 150 years sheds light on the difficulty of the task and the commitment agreed by the countries signatories of the agreement.

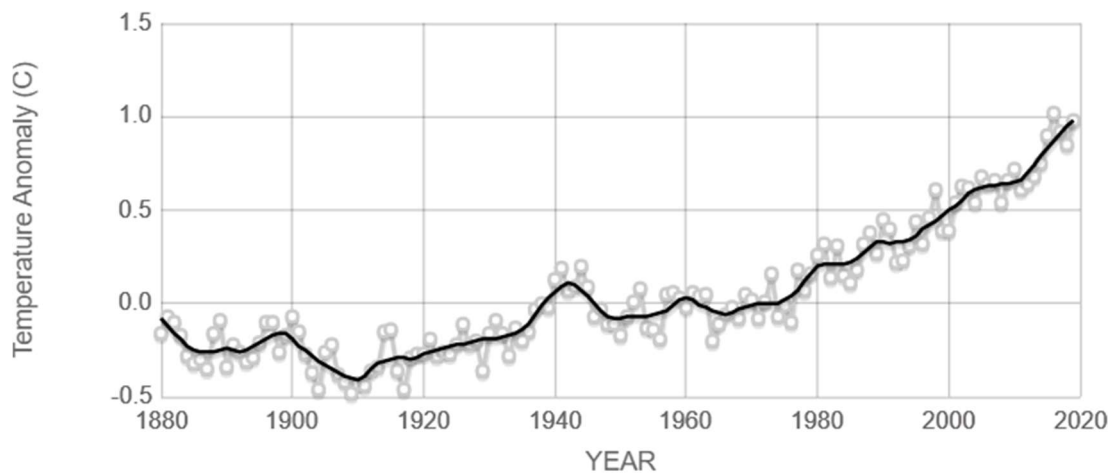


Figure 1. Variation of global temperature [2]

The above presented graph shows the variation of global temperature compared to the average temperature from 1951 to 1980. During the last 50 years, the global average surface temperature has increased over 1°C driven by the equivalent increase in greenhouse gas emissions. Worse than that, it seems the increase has become deeper

during the last years and it shows no weakening whatsoever. Therefore, the commitment signed in the Paris Agreement seems very ambitious given the circumstances. The objectives of GHG emissions reduction have been set in order to reach the global emissions peak as soon as possible. Moreover, the difference in requirements between developed and non-developed countries has been acknowledge, stating they have the right to keep their development towards a welfare level equivalent to that of the developed countries and ,thus, it will take longer for them to meet those objectives.

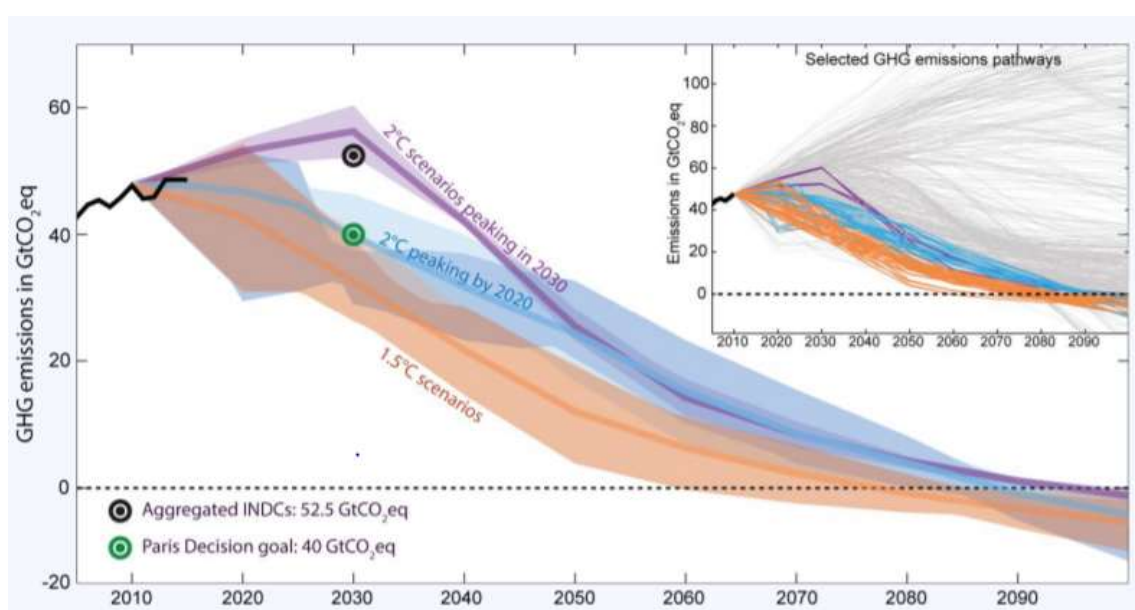


Figure 2. Global Emissions consistent with the Paris Agreement compared to current aggregated pledges [3]

The above presented graph shows the different possible scenarios of GHG emissions in order to meet the objectives signed in the Paris Agreement. Reaching the emissions' peak as soon as possible is key in order to be able to follow a less drastic reduction curve in the future. It is paramount to keep in mind this reduction will not be something abstract, but it will translate into real changes in the way we live. Therefore, it is essential that these efforts are distributed along all the fields available, so that the impact is as mild as possible. Thus, changes must be implemented in all fields of our society, being the

electrical grid one of the elements with the highest potential for the development of new technologies.

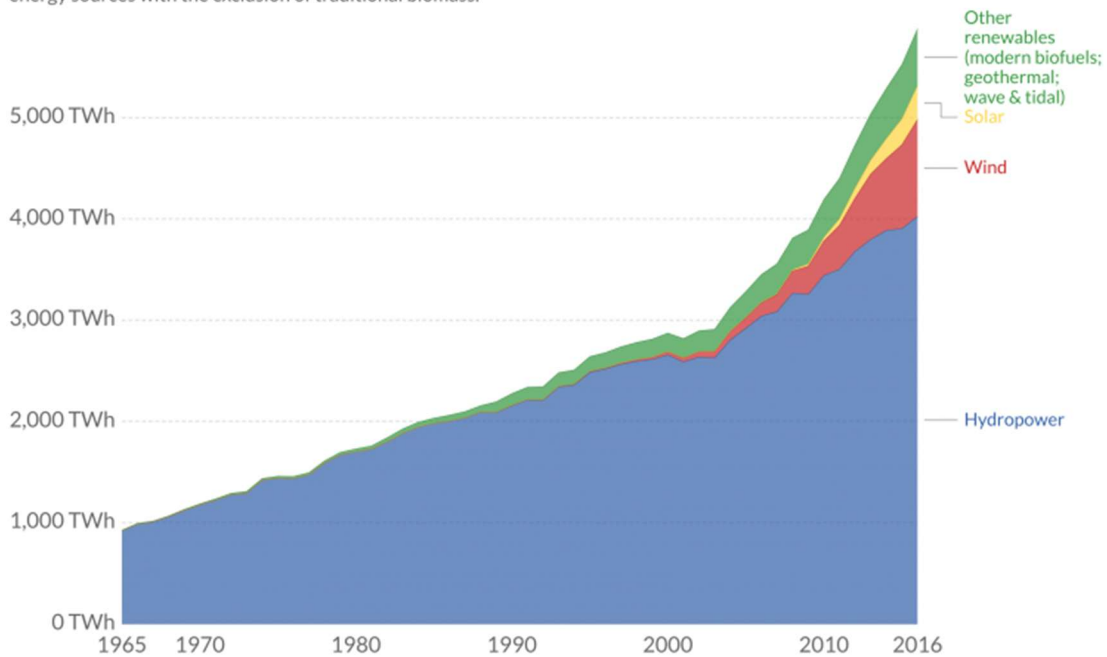
Regarding the Energy Supply System, these changes will be driven by the introduction of Renewable Sources in combination with the enhancement of the Battery Energy Storage Systems that enables an optimal dispatch. Moreover, based on the scenarios presented in Figure 2, they suggest society must become carbon negative by the end of the century, which means not only reducing our emissions but also removing GHG already in the atmosphere. Therefore, it can be stated that Negative Emissions Technologies will play a main role in the power grid, acting jointly with RES and BESS in order to achieve sustainability.

1.1.2. Challenges of the Implementation of Renewables

Renewable Energy Sources are the alternative to Conventional Sources, which imply emissions of one of the main GHG: carbon dioxide. These new sources, principally led by solar, wind and hydro, are increasingly being implemented in many countries in order to address the challenge of global warming. Specifically, wind and solar have experienced a great development during the past two decades, and its presence in society's energy mix has increased significantly.

Modern renewable energy consumption, World

Total renewable energy consumption, measured in terawatt-hours (TWh) per year. This data includes all renewable energy sources with the exclusion of traditional biomass.



Source: BP Statistical Review of Global Energy

CC BY

Figure 3. Modern Energy Mix [4]

The introduction of solar and wind energy has enabled many countries to begin their transition towards a more sustainable energy supply system. However, these two energy sources add variability to the power generation, which poses a threat to the operation of the grid. The difficulties to predict the availability of these two resources derives from the challenge of forecasting the weather conditions, which added to changes in demand can cause problems for the operation of the grid and for the energy markets.

Problems regarding energy markets have already happened. This is the case of Germany, a country that has undertaken a very ambitious plan under the name “Energiewende” which aims to fulfill their transition towards a sustainable energy supply system. Nevertheless, the country’s energy market has already experienced curious phenomenon such as the one of last December, when the energy price of the German market EPEX Spot Deutschland became negative.

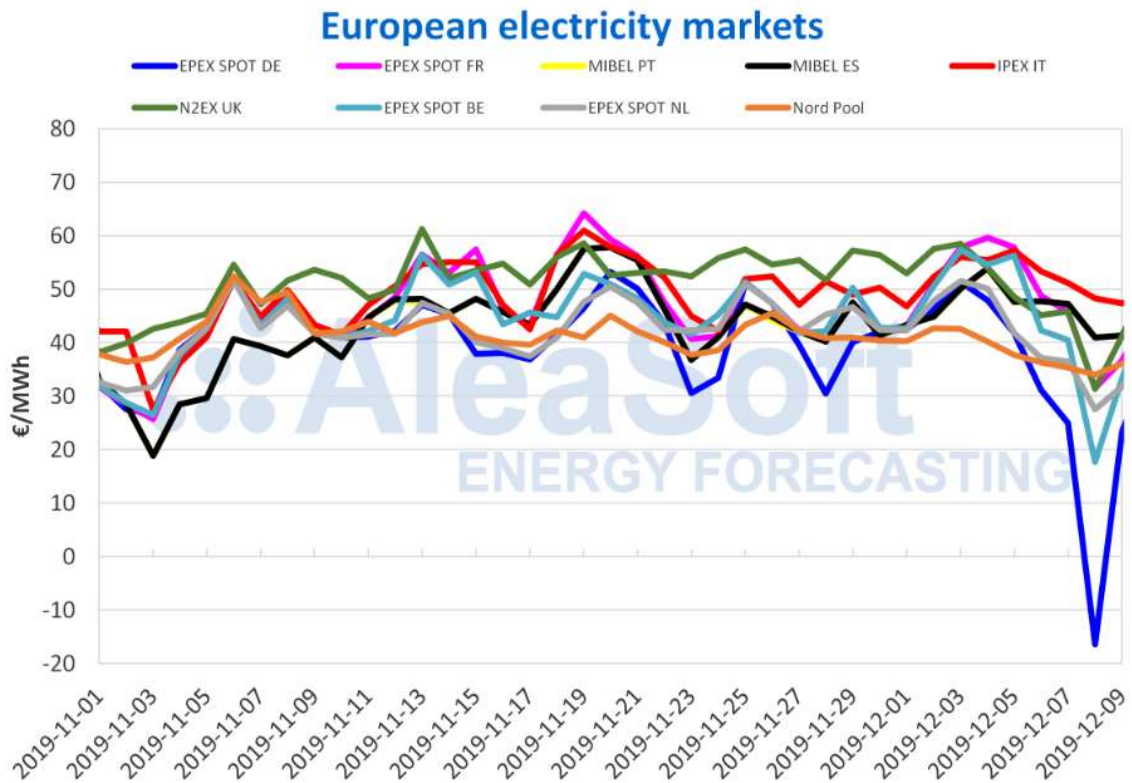


Figure 4. European electricity price, November-December 2019 [5]

This was the consequence of a low demand period combined with strong winds which provided a surplus of wind power in the grid. This exemplifies what challenges can arise from the implementation of renewables and its coordination with the demand in the grid. On the other hand, solar energy poses challenges to the system from a different perspective. Sudden changes in solar availability due to cloud coverage affect the planning and operation of the grid. Moreover, the main potential of solar energy is its implementation as Distributed Generation, which consists of installing solar panels on the roof of the households. DG implies turning traditional consumers to occasional generators which can cause events such as reverse power flow and overvoltage.

This study focuses on the implications of solar energy as DG in combination with BESS by assessing the challenge of designing voltage controls which could ensure an optimal dispatch of the BESS and the PV units. In order to achieve so, this research project follows the schematic proposed in [6].

1.2. Objective

The aim of this study is a two-fold objective. First, an OPF is proposed in order to minimize the carbon footprint of a certain distribution network. This is a centralized offline power flow which allows the creation of a database of optimal generation setpoints of the distributed solar panels and optimal injection curves for the BESS. Once the database is complete, it serves as the basis for the second part of the study: the voltage control design. Building on the previous step, local voltage controls are designed by means of linear regression. Last, these controls are tested in order to evaluate their performance.

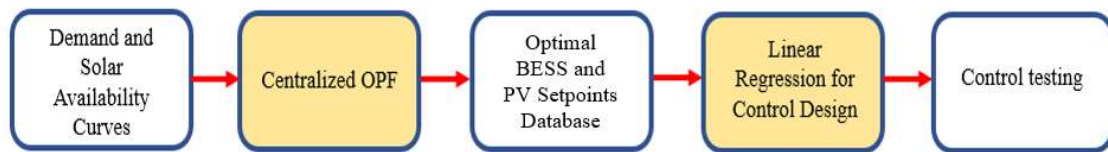


Figure 5. Structure of the study

1.3. Overview

This research study is structured as follows: next chapter contains a discussion of how the voltage control task is performed today, and what changes can be expected in the sector. Section 3 describes the methodology proposed and the steps that link the different stages of the study. Chapter 4 holds a discussion of the results obtained for both the base case and the case study. Then, section 5 develops an economic and environmental assessment based on the results obtained in the previous chapter. Last, in chapter 6 conclusions about the results and the methodology are drawn, as well as a discussion of potential future works related to the subject.

2. State of the Art

This second chapter of the study aims to provide a general overview of how the task of voltage control is carried out nowadays in the industry and what the main potential innovations in the field are.

2.1. Voltage Control Today

The objective of voltage control is to maintain the voltage magnitude of all the buses in the network within their safety limits. This task, joined with the frequency control, are the two main challenges that operators of the grid must solve in order to provide a safe and reliable power system to the consumers. Achieving an optimal dispatch while respecting the equipment limitations is the ultimate goal of grid operation.

Focusing on the task of voltage control, nowadays there exist several techniques that participate in the process: excitation control at generating stations, tap changing transformers and shunt reactors and capacitors.

First, voltage regulation via excitation control at generating stations is effective in short lines. An automatic voltage regulator is installed in the generator and compares the measured voltage with the reference value. This voltage error is corrected by modifying the excitation current and, therefore, the excitation voltage. This allows to compensate the voltage drop caused by load variations and obtain the desired voltage. Below presented is the structure of this type of control:

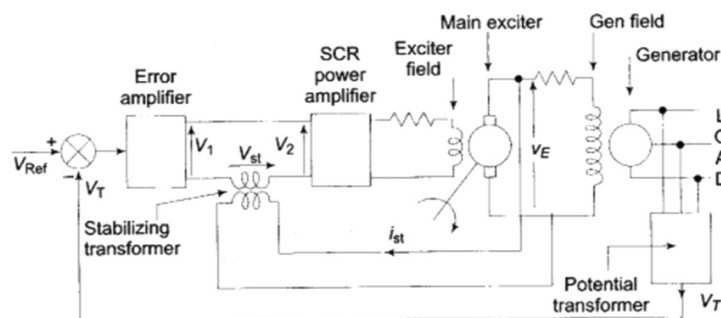


Figure 6. Automatic Voltage Regulator for Generating Stations [7]

However, the most extended technology to control the voltage in both transmission and distribution networks are the tap changing transformers. By changing the number of turns

ratio of the transformer, the voltage of the secondary experiences a proportional variation to that exerted in the turns ratio. There are transformers that only allow this change after being disconnected from the load. These are known as off-load tap changing transformers and, although they are cheaper, the power supply interruption they cause every time they try to perform a voltage control action deteriorates the quality of the service provided. On the other hand, there exist transformers that do not cause this kind of interruptions: the on-load tap changing transformers, which are more extended in the modern network for their ability to guarantee continuity of the supply.

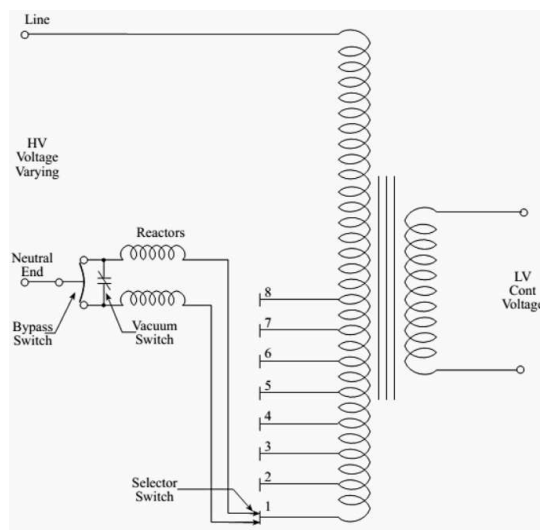


Figure 7. On-Load Tap Changing Transformer [8]

There is also the possibility of utilizing shunt devices in order to regulate the amount of reactive power flowing through the grid. On the one hand, shunt reactors are inductive elements which are normally installed in transmission lines. During low demand periods, lines tend to generate reactive power, that is they acquire a capacitance behavior, which leads to increases in the voltage. By connecting the shunt reactors, this capacitance is compensated and the voltage is controlled. On the other hand, shunt capacitors come into play when the current is too inductive (e.g. in industrial loads) and try to compensate this reactance.

These technologies are the most extended in today's standard of grid operation. Most of the control decisions are made from a centralized approach, that is from the ability of

accessing all the information about the grid's state and planning its dispatch accordingly. However, new technologies have brought distributed generation as the potential reality of the power supply systems and, therefore, setting new challenges that question if a certain decentralization would be necessary in order to address the new requirements.

2.2. Centralized, Decentralized and Distributed Control

The development of new technologies, led by the introduction of DG, is changing the paradigm of the power supply sector. The traditional paradigm of a single direction flow, where the power flows downstream from the big generators to the consumers, will be affected by the introduction of solar panels as a consumer option to produce its own energy. This joined with the introduction of BESS will change the established relationships in the sector and will make necessary to reconsider the actual standard of operation.

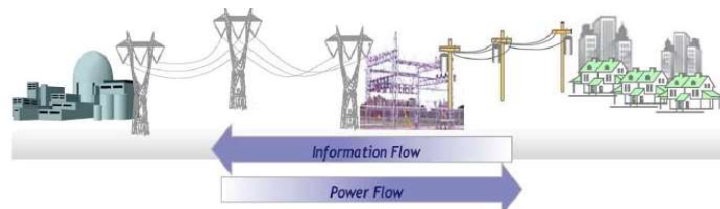


Fig. 2. Power and information flow in the traditional power system environment [13]



Fig. 3. Power and information flow under the smart grid environment [13]

Figure 8. Paradigm Shift of the Power Supply Grid [9]

The actual standard of operation is characterized by a deep centralization of the information processing and the decision-making process. Such process requires a vast, robust and expensive communication infrastructure that ensures a continuous and effective control of the grid. Therefore, DNs operate as passive elements that provide information to the central control, which processes the data in order to find the optimal dispatch for the whole network. However, this approach does not benefit from the flexibility provided by the DERs and struggles to solve the challenges proposed by the new technologies [6].

On the other hand, decentralized control employs local measurements in order to obtain the optimal without the need of building a communication infrastructure. However, this approach could lead to inefficiencies and reliability issues in a fast-changing environment [6].

Last, the distributed approach tries to combine the two strategies above presented, by harnessing the flexibility of local measurements while relying on a certain degree of centralization via communication infrastructure. It is predictable that the future of the grid will resemble the distributed approach in order to face the challenges set by the introduction of the new technological developments.

2.3. The Future of Grid Operation

The grid is a producer of massive data: generations, demands, voltages magnitudes... All these measurements are performed continuously during the operation of the grid, which provides large sets of data that record the historical behavior of the grid. Until now, the sector did not possess the technology needed to process this data and fully harness its potential for the operation of the grid. However, with the development and enhancement of Machine Learning techniques, the implementation of local control strategies that tackle more efficiently the challenge of operation seems more feasible than ever. In fact, there are many who have already developed and proposed different data-driven models that could accurately represent certain scenarios of the grid and that could perform an effective control of it.

This is the case of [10], where they develop an Input-Output model so that a certain distribution network can provide a given amount of active power to the main grid. The proposed methodology relates the active injection of the DERs of the DN and the power delivered by the DN to the bulk system. Moreover, they provide means to estimate the parameters of the model and a control to perform the task while minimizing the generating costs. They run several simulations in order to test the performance of the proposed methodology. For instance, they simulate the congestion of a line while keeping constant the amount of power delivered to the bulk system. As shown in the graph below, the DER placed near that line (bus 56) decreases its generation, while the rest increases it in order to maintain the delivered power.

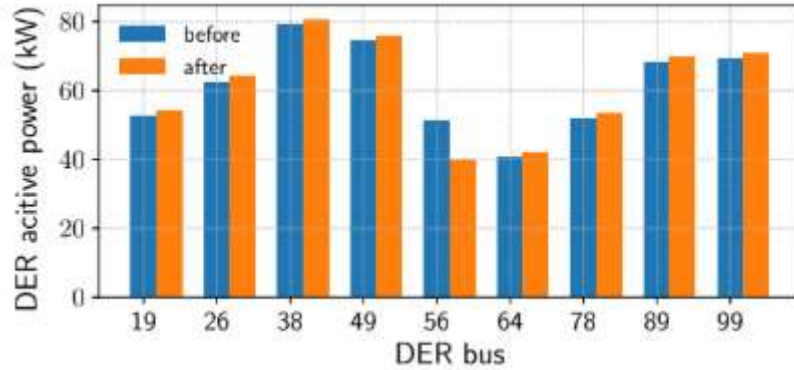


Figure 9. Response to line congestion [10]

Other papers, such as [6], provide a framework where centralized and decentralized data-driven techniques are implemented. They propose a centralized OPF based on historical consumption data that provides the optimal dispatch of the grid. The data generated during this process is then organized in database of optimal setpoints that underpins the design of local controls. These decentralized controls are the result of applying ML techniques, such as regression. Moreover, another innovative aspect of this paper is the introduction of the so-called chance constraints, that represent the uncertainty introduced by DERs. Monte-Carlo simulations, Kernels... are some of the techniques developed in that paper.

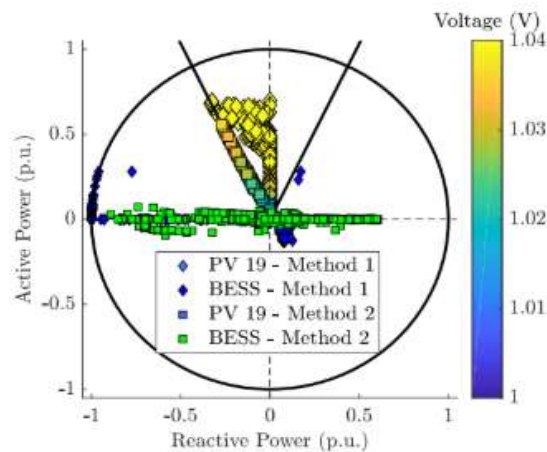


Figure 10. BESS Data-driven Local Control [6]

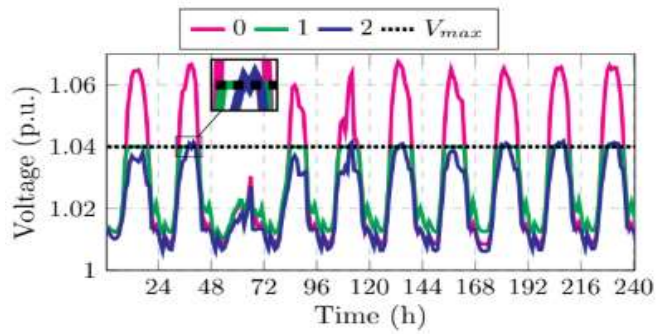


Figure 11. Comparison of performance between Centralized and Local Control [6]

Figure 10 represents the control designed for the BESS, while figure 11 shows the comparison between the voltage profile obtained with the centralized OPF (1, optimal behavior) and the profile obtained after the simulation of the performance of the local controls (2, control response).

These papers show the potential of data-driven techniques for the design of complementary local controls that could enhance the response of the grid to the new challenges. This is the main motivation of this paper, which aims to be an initial step towards the development of further research.

3. Model Description

As already stated, the study consists of two separate sections. First, an optimal power flow is developed in order to create a data base of optimal generation setpoints that underpins the following section, in which voltage controls are designed by utilizing the obtained data and ML techniques. The objective of this chapter is to present and explain the theoretical background behind the proposed model and clarify the steps that link the different stages of the methodology.

3.1. Centralized Optimal Power Flow

In this study a centralized OPF is developed in order to minimize the carbon footprint of the network in analysis. The cost function is subject to a given set of constraints that defines the characteristics of the problem. For the purpose of this research, the constraints of the power flow itself are defined by the DistFlow model of the grid. The DistFlow representation is a way of eliminating the complex aspect of the electrical dynamics that remains accurate for radial distribution networks. By erasing the angles of both voltages and currents phasors, the solution of the problem becomes feasible (implementation of code in Appendix E).

3.1.1. Multiperiod characteristics

This study aims to optimize the generations of the given network during a certain period of time by operating with generation and consumption elements whose timely performance is key for such purposes. Therefore, the constraints and the cost function must include a multiperiod aspect that reflects such attribute.

3.1.2. Objective function

The final purpose of this algorithm is to minimize the carbon footprint of the power consumed in the network studied. The variables that should be included in such carbon cost function are the generations of the non-renewable resources, which capture both the consumption and the losses. The objective function is presented below:

$$\min \sum_{t=1}^{T_{hor}} \left\{ \sum_{n=1}^N (Eg_t * Pg_{n,t}) \right\} * \Delta t \quad (1)$$

There are two sets included in the shown function: T and N , which are identified by the indexes t and n , respectively. T represents the set of time, and N , the buses. $P_{g_{n,t}}$ is the active power generated by unit n in time t ; E_{g_t} is the carbon intensity coefficient of the grid during time t . The last element in the function, Δt , represents the length of the period of operation.

The cost function proposed is a single objective function since it only contemplates the generations. Simplifying the objective of the cost function eases the optimization process and eliminates the discrepancies present in multiobjective models. This is exemplified by the problems experienced when trying to unify the cost aspect of generation and losses, which can produce meaningless objective values.

3.1.3. Decision variables

The variables that define the cost aspect of this problem are the active power generations, namely $P_{g_{n,t}}$. The rest of the variables, e.g. voltages, currents, and reactive generations, are intermediate variables that complete the definition of the problem with the restrictions imposed.

3.1.4. DistFlow Model

The DistFlow equations is a relaxation of the conventional power flow equations suitable for radial distribution networks. Rather than performing calculations with phasors, this model employs the square magnitude of the network voltages and currents. Upon achievement of the solution, the phasorial aspect of these variables can be recovered. Nevertheless, for the purpose of this study the recovery of the phasors angles is only of interest to compare the performance of the proposed OPF to other conventional power flows. Angles do not interfere in the second part of the study.

Basing on the Branch Flow Model, the DistFlow Model provides a relaxation that eliminates the complex side of the equations, transforming the branch flow as follows:

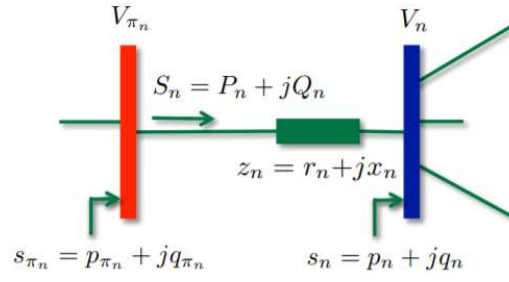


Figure 12. Branch Flow Model Schematic [11]

In order to erase the complex aspect this schematic yields, the relaxation performed by utilizing the square magnitudes of the phasors, adapted to the notation of this study, is the following:

$$l_{j,t} = |I_{j,t}|^2 \quad (2)$$

$$v_{n,t} = |V_{n,t}|^2 \quad (3)$$

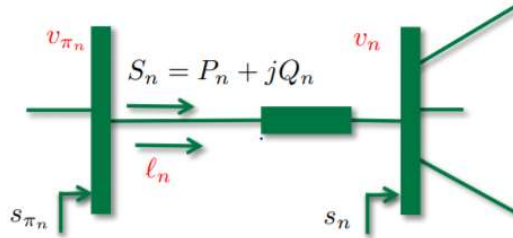


Figure 13. DistFlow Schematic [11]

This relaxation modifies the optimization problem by providing new power flow constraints that enable the problem to be solved. The model establishes relationships between voltages, currents and power as follows:

$$v_{n,t} = v_{\pi_n,t} - 2r_n P_{j,t} - 2x_n Q_{j,t} + (r_n^2 + x_n^2) * l_{j,t} \quad (4)$$

$$\frac{P_{j,t}^2 + Q_{j,t}^2}{v_{\pi_n,t}} = l_{j,t} \quad (5)$$

$$\sum_{k:n \rightarrow k} P_{k,t} = p_{n,t} + P_{j,t} - r_n l_{j,t} \quad (6)$$

$$\sum_{k:n \rightarrow k} Q_{k,t} = q_{n,t} + Q_{j,t} - x_n l_{j,t} \quad (7)$$

Being $P_{j,t}$ and $Q_{j,t}$ the power in each branch j ; $v_{n,t}$ the predecessor bus voltage; $P_{k,t}$ and $Q_{k,t}$ the power through the branches connected to the feeding bus. The remaining terms, $p_{n,t}$ and $q_{n,t}$, are the power injections in bus n in time t . The equation below shown models the injection of buses without BESS, thus, they are simply defined by the demand and generation in each node:

$$p_{n,t} = Pg_{n,t} - Pd_{n,t} \quad (8)$$

$$q_{n,t} = Qg_{n,t} - Qd_{n,t} \quad (9)$$

For the purpose of this research, reverse power flow is allowed. Thus, no restriction is applied to the value of branch flows.

3.1.5. Energy Sources generation limits

Depending on the type of source energy, each generator fixes a set of constraints regarding their limits of operation. Each of them has an upper and lower limit that must be respected in order to produce a feasible solution. For the conventional energy sources, this set of restrictions looks as follows:

$$Pg_c^{min} \leq Pg_{c,t} \leq Pg_c^{max} \quad (10)$$

$$Qg_c^{min} \leq Qg_{c,t} \leq Qg_c^{max} \quad (11)$$

Being C the subset of nodes with conventional generation. On the other hand, the PV units' generation limits have a dynamical aspect, that is they depend on the availability of solar energy in each period of time. This availability is provided in kW/m²; thus, a surface coefficient is added depending on the power of the node with solar panels. Such coefficient is explained in section 3.3. Furthermore, the reactive generation of solar panels is neglected in this study in accordance with the general operating standard for this kind of DG elements.

$$0 \leq P_{g_{r,t}} \leq Avail(t) * Surfcoef_r * P_{g_r}^{max} \quad (12)$$

Being R the subset of nodes with PV units installed.

3.1.6. Branch currents and bus voltages limitations

There are constraints set by thermal limitations and overload capabilities. In this case, since the problem is modelled using the DistFlow equations, these restrictions are referred to the square magnitude of both the branch currents and the bus voltages.

$$0 \leq l_{j,t} \leq l_j^{max} \quad (13)$$

$$v_n^{min} \leq v_{n,t} \leq v_n^{max} \quad (14)$$

3.1.7. Energy Storage Systems

The implementation of Energy Storage Systems is paramount for performing a meaningful optimization that ensures a complete utilization of the renewable resources. The objective is to harness two different situations: first, use the surplus of solar energy during low demand periods to meet the demand during other periods; second, benefit from the variable carbon intensity of the grid. The equations that model the batteries have been retrieved from [6] and adapted to meet the requirements of the optimization problem.

The first aspect to introduce in the model is a constraint that ensures the battery is not charging and discharging at the same time. The constraint that defines this behavior includes the charging of the battery, $Pch_{b,t}$, and the discharging, $Pdis_{b,t}$, as positive variables.

$$Pch_{b,t} + Pdis_{b,t} \leq \max(Pch_{b,t}, Pdis_{b,t})$$

Being B the subset of nodes with energy storage capability. However, in order to introduce this constraint in the model, it has to be formulated in a way manageable for the solver. Therefore, two binary constraints are introduced in the model: $xch_{b,t}$, which has the value of 1 whenever the battery is charging, and 0 otherwise; and $xdis_{b,t}$, which behaves the same way as the previous binary variables but representing the discharging. In order to avoid simultaneous charging and discharging, these variables are related with the following constraint:

$$xch_{b,t} + xdis_{b,t} \leq 1 \quad (15)$$

These binary variables accompany their corresponding charging and discharging continuous variables in the rest of the constraints. The second aspect to introduce in the model is a modification of the active injection equations for the buses where the PV are installed, in order to consider the charging and discharging of the batteries in each period of time. It is worth noting that, although the battery can be charged from two different sources, the charging is modelled with a single variable. This means that both the charging from the grid and the charging from the solar energy surplus are represented with the variable $Pch_{b,t}$. The charging must be introduced in the injection equations with a minus sign since it can be thought of as a demand. On the other hand, the discharge, $Pdis_{b,t}$, is included in the injection equation as positive since it can be thought of as a generation. The values of these variables are defined as positive, from zero to the specification of maximum power of the battery:

$$p_{b,t} = Pg_{b,t} - Pd_{b,t} + xdis_{b,t} * Pdis_{b,t} - xch_{b,t} * Pch_{b,t} \quad (16)$$

$$0 \leq Pch_{b,t} \leq Pch_b^{max} \quad (17)$$

$$0 \leq Pdis_{b,t} \leq Pdis_b^{max} \quad (18)$$

On the other hand, for the purpose of this research, the reactive generation of the battery is neglected. This neglect of the reactive aspect of the battery follows the established standard in grid operation. Recent developments show the possibility of harnessing the reactive aspect of energy storage systems for voltage control purposes. Nevertheless, this application is out of the scope of this study.

In order to accurately model the behavior of the battery, an energy description must be developed through additional constraints. An initial energy level is set, and, throughout the day, it is updated following the charging and discharging of the battery defined by equation (22). The maximum energy capacity of the battery is limited by the specified upper bound of the device and the efficiency of the battery is considered. A lower bound must also be included. Batteries used in combination with solar panels should not be discharged completely in order to lengthen their useful life. This parameter is called Depth of Discharge (DoD), and limits the minimum amount of energy that must remain at all time in the battery [12]:

$$Ebat_{b,1} = Einitial \quad (19)$$

$$Ebat_{b,t} = Ebat_{b,t-1} + \left(xch_{b,t} * \eta * Pch_{b,t} - xdis_{b,t} * \frac{Pdis_{b,t}}{\eta} \right) * \Delta t \quad (20)$$

$$(1 - DoD) * Ebat_{cap} \leq Ebat_{b,t} \leq PU_{limit} * Ebat_{cap} \quad (21)$$

In equation (22), Δt refers to the granulation of the problem, which in this case is 10 minutes. PU_{limit} is the per unit limit of the battery, which multiplied by the battery capacity yields the upper bound of the energy variable. Furthermore, another additional constraint is provided to better define the behavior of the battery. It only makes sense that the battery utilizes all the energy it has been able to store throughout the period of operation, so that the solution obtained can be fully optimal. Therefore, the final energy value must be equal to the initial value, which implies that the next day the battery should start at the same energy level as the previous one.

$$E_{bat_{b,end}} = E_{\text{initial}} \quad (22)$$

The battery used is the Powerwall designed by Tesla. Specifications are in Appendix D.

3.1.8. Complete OPF

Below presented is the summarized optimization problem of this study. Spyder [13] has been used for the modelling of such formulation and as a solver, Gurobi [14].

$$\min \sum_{t=1}^{T_{hor}} \left\{ \sum_{n=1}^N (Eg_t * Pg_{n,t}) \right\} * \Delta t$$

s.t.:

$$\begin{aligned} l_{j,t} &= |I_{j,t}|^2 \\ v_{n,t} &= |V_{n,t}|^2 \\ v_{n,t} &= v\pi_{n,t} - 2r_n P_{j,t} - 2x_n Q_{j,t} + (r_n^2 + x_n^2) * l_{j,t} \\ \frac{P_{j,t}^2 + Q_{j,t}^2}{v\pi_{n,t}} &= l_{j,t} \\ \sum_{k:n \rightarrow k} P_{k,t} &= p_{n,t} + P_{j,t} - r_n l_{j,t} \\ \sum_{k:n \rightarrow k} Q_{k,t} &= q_{n,t} + Q_{j,t} - x_n l_{j,t} \\ p_{n,t} &= Pg_{n,t} - Pd_{n,t} \\ q_{n,t} &= Qg_{n,t} - Qd_{n,t} \\ Pg_c^{min} &\leq Pg_{c,t} \leq Pg_c^{max} \\ Qg_c^{min} &\leq Qg_{c,t} \leq Qg_c^{max} \\ 0 &\leq Pg_{r,t} \leq Avail(t) * Surfcoef_r * Pg_r^{max} \\ 0 &\leq l_{j,t} \leq l_j^{max} \\ v_n^{min} &\leq v_{n,t} \leq v_n^{max} \\ p_{b,t} &= Pg_{b,t} - Pd_{b,t} + xdis_{b,t} * Pdis_{b,t} - xch_{b,t} * Pch_{b,t} \\ 0 &\leq Pch_{b,t} \leq Pch_b^{max} \\ 0 &\leq Pdis_{b,t} \leq Pdis_b^{max} \\ xch_{b,t} + xdis_{b,t} &\leq 1 \\ Ebat_{b,1} &= Einitial \\ Ebat_{b,t} &= Ebat_{b,t-1} + \left(xch_{b,t} * \eta * Pch_{b,t} - xdis_{b,t} * \frac{Pdis_{b,t}}{\eta} \right) * \Delta t \\ (1 - DoD) * Ebat_{cap} &\leq Ebat_{b,t} \leq PU_{limit} * Ebat_{cap} \\ Ebat_{b,end} &= Einitial \end{aligned}$$

3.2. Load curves

Commonly, offline OPF algorithms are supported by historical consumption data of the grid in study. Thus, the model is able to represent with higher accuracy what the future situation of the grid will be. By having a fair approximation of the behavior of the loads depending on the hour, the day and the season, the model yields solutions closer to the actual behavior.

For this research, since the network information has been obtained from the Matpower library [15], such historic demand data is not available for the user. Instead of using historical data of the network, load curves are introduced in the problem in order to model the demand behavior. Three types of curve are used depending on the consumption they represent: residential, industrial and commercial. These curves have been obtained from [16]. They present a one-minute granulation, so in order to adapt them to the purpose of this research, the curves are divided in groups of ten moments of time and the mean of such groups is representative of such periods of time. Thus, the granulation of the curves is changed from 1440 points to the intended 144.

This section is intended to present and clarify the differences between the various types of consumers connected to the network and the reasons of these characteristics from two different perspectives: first, the variation in demand throughout the day, and second, the differences in the demand profile depending on the day of the week.

3.2.1. Household consumption

Residential consumption has unique characteristics that pose a challenge when trying to coordinate the generation of solar panels installed in the residences and the household electricity demand. Below presented is a three-day residential load curve:

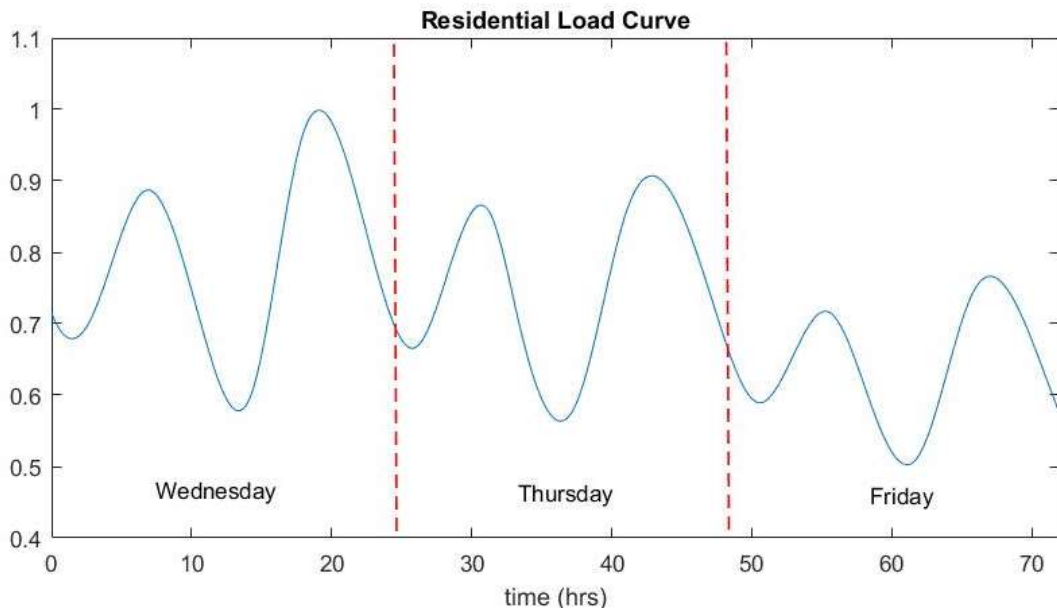


Figure 14. Household demand

Figure 3 offers a representation of the evolution of the electrical demand in a household. In this curve, the following can be observed: two peaks and two valleys define this trend by following each other alternatively. First, a period of nearly constant low demand is presented during the time when the residents are asleep. Then, a peak is observed that corresponds to the moment when the residents connect many of the domestic appliances to start their day. Following this peak in demand, a deep valley appears when residents leave their homes during working hours. Last, the returning of the residents to their households results in a peak in demand during the last part of the day. On the other hand, differences between the days are not very remarkable beyond a decrease in general consumption from Wednesday to Friday.

3.2.2. Industrial consumption

The industrial demand curve is presented below. It can be observed the tendency differs from the residential load curve.

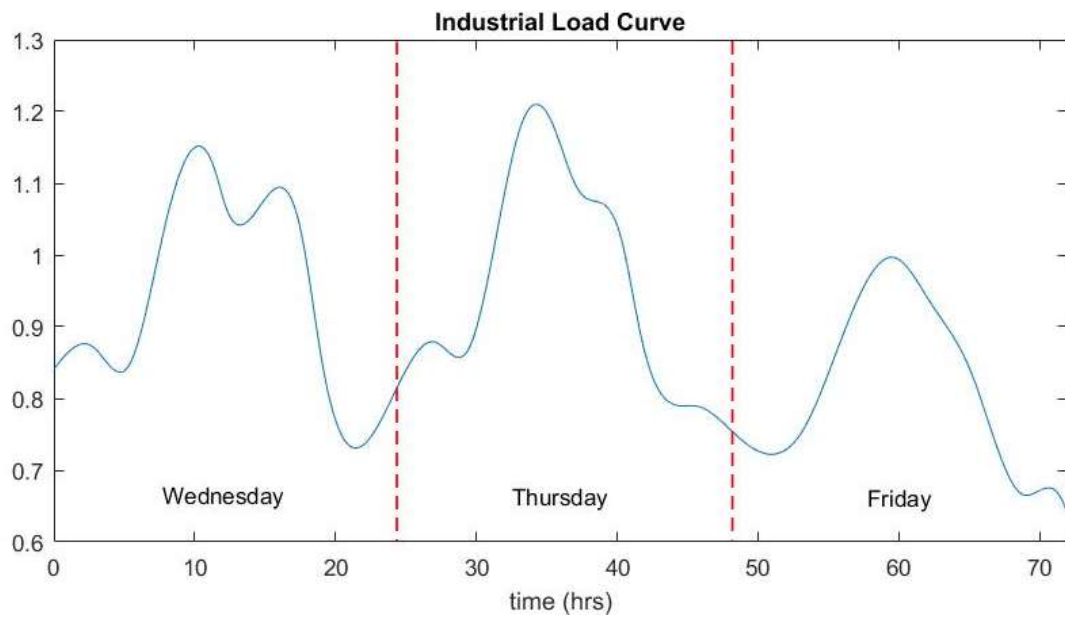


Figure 15. Daily industrial demand

From comparing Figure 3 and Figure 4 Wednesday's period, essential differences between the two can be observed. In the case of the industrial demand, it presents one main peak at 9:00am, which corresponds to the initiation of the working activities. The rest of the curve develops around this peak with decreasing values throughout the day and a less sharp peak at 4:00pm. The magnitude of the curve throughout the day suggests that industrial processes are more energy intensive than the residential consumption. However, the decreasing tendency in consumption from Wednesday to Friday mirrors the one from the household curve. It is also worth noting the peaks in demand during the beginning of both Wednesday and Thursday, which could correspond to industrial facilities performing its activity during hours when the price of electricity is the lowest in the day.

3.2.3. Commercial consumption

The last demand model introduced in the problem is the commercial load shown below.

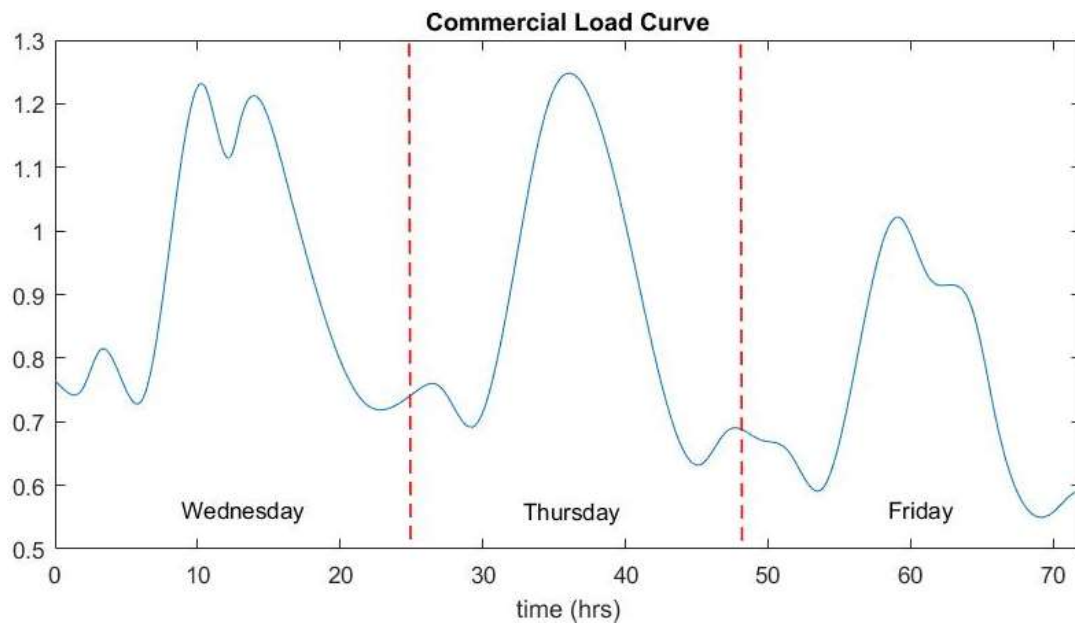


Figure 16. Daily commercial demand

The commercial curve mirrors better the industrial curve rather the residential one. A main peak appears at noon, with differences depending on the day. As well as the industrial curve, the commercial demand reveals a soft peak in consumption during the last hours of the day, which could correspond to night commercial activities. Furthermore, the decreasing tendency in consumption from Wednesday to Friday revealed in the two previous graphs, appear in the commercial curve as well.

3.3. Solar Availability Curve

The proposed model also captures the dynamic aspect of the photovoltaic generation. Therefore, unlike the CES, the generation capacity of the PVs varies between the different time periods following a curve that considers the variation of available solar energy throughout a day. The aforementioned curve is shown in the graph below:

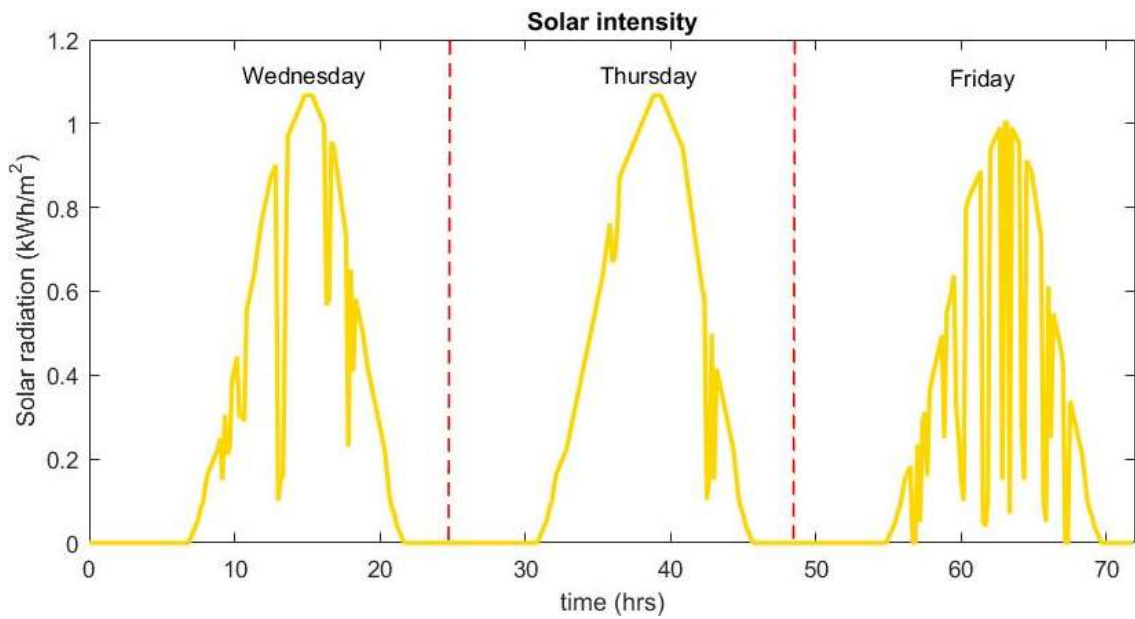


Figure 17. Daily variation of solar radiation

The proposed radiation curve aims to provide a realistic model of the available solar energy during a late spring day in a region located around the 40th parallel north, capturing sudden changes due to cloud coverage. This local aspect is reflected in the hours between which there is solar availability, that is the sunrise and the sunset, which are fixed to be 7:00am and 9:30pm, respectively. The magnitude of the curve is based on the daily average solar radiation in the area of Madrid during June, which reaches a total of 8 kWh/m² per day, with 8.5 kWh/m² and 6.9 kWh/m² as the 75 and 25 percentiles, respectively [17].

Type of day	Solar Intensity (kWh/m ²)
Sunniest (Percentile 75)	8.5
Average (Mean)	8
Cloudy (Percentile 25)	6.9

Table 1. Day type attending to solar radiation

Since the availability is provided per unit of surface, it is necessary to establish a standard to define the capacity of a certain node. Assuming the average household power is around 5 kW, every 0.1 MW of residential demand corresponds to 20 households, each of which are assumed to have an available surface for solar panels of 6 m².

No reactive generation will be considered in this study for the PV units. This decision, as well as the decision to neglect the reactive generation of batteries, is discussed in the battery model section.

3.4. Grid's Carbon Intensity Curve

In order to accurately capture the dynamic aspect of emissions throughout a day, a carbon intensity curve is introduced in the model. The carbon intensity of a grid varies depending on several factors, such as season, day, hour, location, etc. Therefore, it is essential to select the adequate curve for the conditions of the given problem. Thus, the curve chosen is the evolution of the carbon intensity in the Spanish grid from the 22nd to the 24th of April 2020, attending to the season criterion already explained for the solar availability curve. Such data has been obtained from [18]. The data available has a granulation of 15 minutes and the intensity for this region is recorded every hour. Therefore, expanding such curve to the required granulation is straightforward.

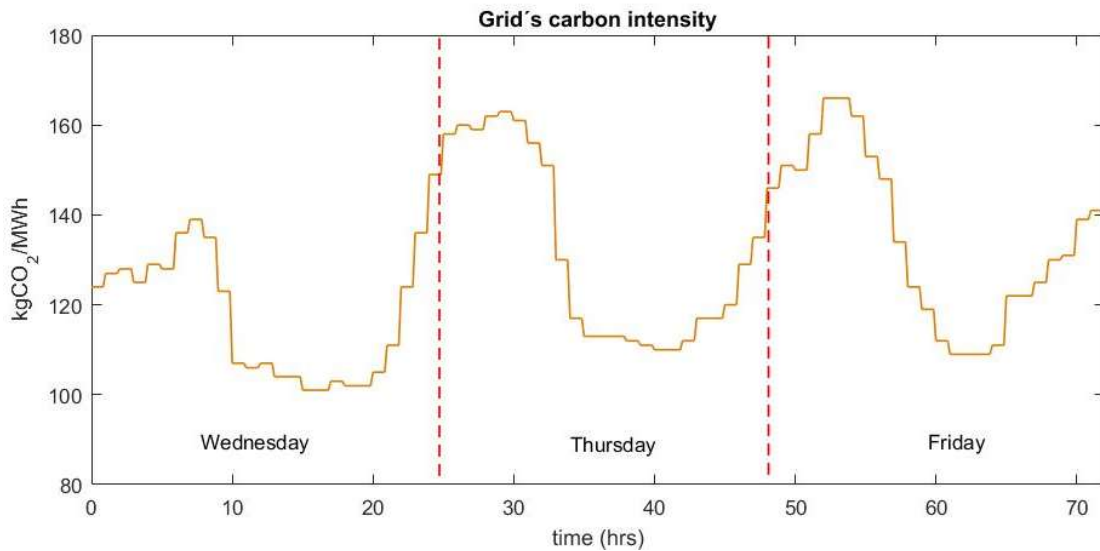


Figure 18. Carbon Intensity of the Spanish Grid

The above presented curve reveals the evolution of the characteristics of the generation in the Spanish grid throughout three spring days. The Spanish Electrical Grid has a relevant penetration of renewable sources due to the weather conditions of the country. The impact of renewables can be observed in the main valley of the carbon intensity curve from 10am to 9pm, where the wind and solar generation leads the renewables to a 60% of the generation share in the country. On the other hand, the main peak in intensity observed around 7am coincides with the peak in demand related to the early hours of the day, and the lack of solar energy during this period. This peak in intensity is caused by the connection of natural gas stations when the renewable generation drops.

Moreover, it also worth noting the difference in magnitude between the days. Although the three days show the same profile, the intensity on Thursday and Friday is higher than on Wednesday. The solar radiation during these three days was very similar, however, the wind generation dropped during the last two, which caused a bigger increase of the CO₂ intensity during the night.

This curve characterizes the new approach towards electricity generation of certain countries. The penetration of renewable energy reaches values of nearly 65% of the total generation, achieving a remarkable environmental efficiency during certain periods. However, when the introduction of renewables is combined with a rejection of nuclear energy, the intensity at night increases due to the connection of other generators, such as

natural gas stations. This new generation paradigm will define the results obtained in this study.

3.5. Grid's Elements Guide

Below presented is the representation of the different elements considered in this analysis.





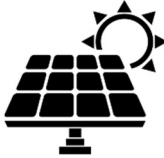

Grid Element	Symbol
Slack	
Residential Consumption	
Industrial Consumption	
Commercial Consumption	
Distributed Solar Generation	
Energy Storage Systems	

Table 2. Grid's Elements Guide

3.6. Local Voltage Control

This section aims to explain the theoretical background that underpins the design and testing of the local voltage controls. Among the various Machine Learning techniques that could be employed, for the purpose of this research, the method selected to build the model is regression. Specifically, in this second part of the study a multivariate regression with quadratic components will be implemented.

3.6.1. Control Design

Local controls try to harness measurements performed in a node in order to control its voltage without the need to utilize a centralized system with costly communication systems. In a data driven approach, these measurements form the set of explanatory variables. After processing this data, the model obtained tries to mimic the real behavior and provide a good estimation for the output: the independent variable.

Regarding the explanatory variables, the measurements that will form this set can be decided prior to the implementation of the regression. In this case, the measurements included will be the bus voltage, the bus demand, the bus PV generation and the BESS energy level. During the process of design, different models will be tested in order to determine which quadratic and linear components should be included and if any should be removed. In order to do so, a coefficient analysis will be performed in order to determine which coefficients are not representative under a minimum level of significance. Correlation coefficient will be evaluated in order to analyze the degree of relation between the explanatory variables and the independent variable.

On the other hand, the two possible variables that could be controlled in each of the buses are the generation of the PV units and the injection of active power of the BESS. The optimal value calculated corresponds to the command given to the control. Regarding the decision of controlling the generation of the PV units, this decision will be made upon analysis of the results provided by the centralized OPF. The reason is that PV generation is controlled by implementing curtailment, which consists of limiting the injection of active power below its maximum level. This decision is made when power from solar sources is redundant in the grid and its injection causes the voltages to increase its

magnitude over the safety limits. Thus, it is only reasonable to control the generation of such devices if the characteristics of the grid lead to situations where the injection of this power could be problematic to the safety of the grid. Otherwise, no control action should be needed, and the solar generation would be equal to its maximum available. BESS injection control, however, is not constrained by this standard. It is worth noting that for the purpose of this research, such injection is considered to be only active power. Although the ability of batteries to provide reactive power could enhance their voltage control potential, the current standard of operation limits their uses to active power producers and consumers.

In order to test the suitability of a regression model, another assessment is needed: the analysis of residuals. This analysis evaluates the performance of the proposed model from a residuals perspective, that is the difference between the observations and the predicted values. A regression model is considered adequate when its residuals possess two principal characteristics: normality and independence. That is the residuals are distributed normally and show a random pattern. However, the quality of this analysis is optimal when the size of the sample is large enough. Therefore, the results of the residual analysis will not be decisive to discard the regression. The performance of the model will be tested with a simulation using a different demand test set.

3.6.2. Control Testing

This second step of the control section is destined to describe the different stages that define the simulation process. In this simulation process, different demand curves will be used in order to test the controls. This demand curves represent the demand during Saturday and Sunday, which correspond to the two following days of the set considered in the design step.

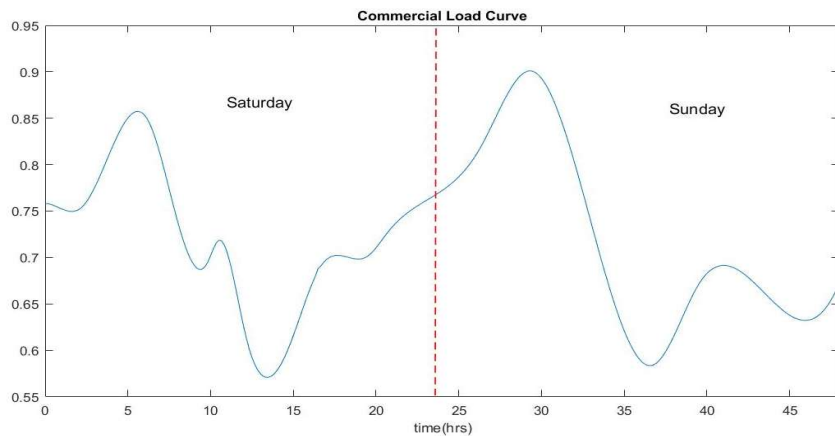


Figure 19. Test Commercial Load Curve

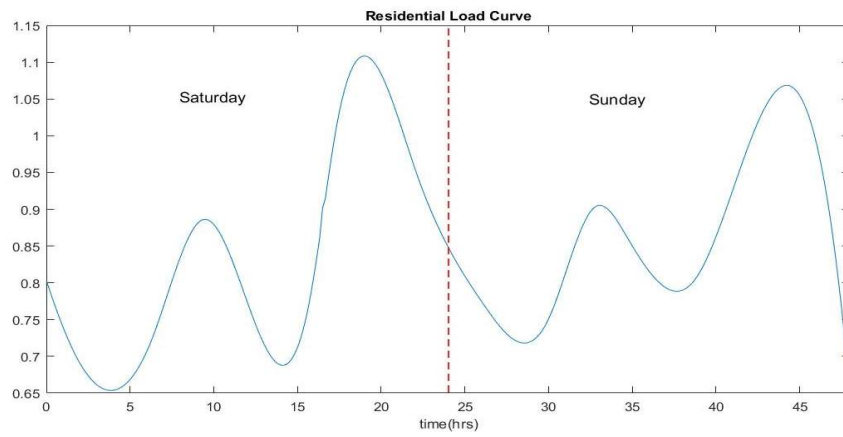


Figure 20. Test Residential Load Curve

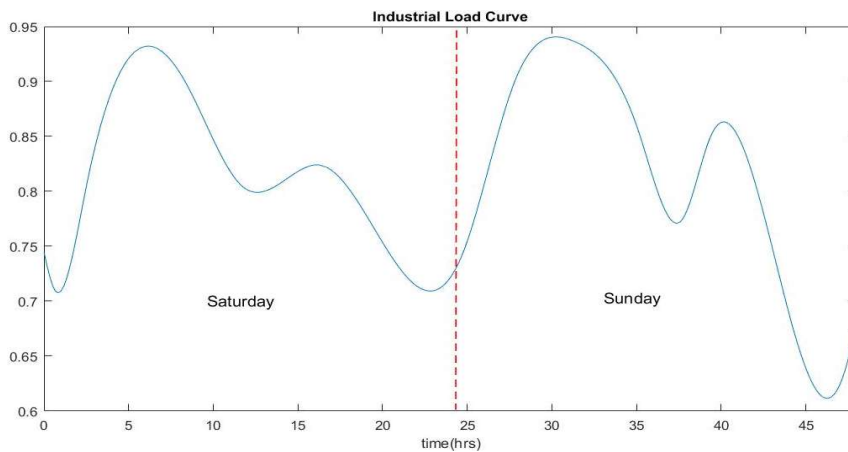


Figure 21. Test Industrial Load Curve

The simulation process consists of the following steps (implementation of simulation code in Appendix F):

- First, it is necessary to obtain the initial solution provided by the centralized OPF. This way, the solution obtained with the controls can be compared to what is considered fully optimal.
- Next, the measurements obtained are introduced in the control so that the optimal output can be calculated. It is important to limit the output of the control so that the estimated value is consistent with the state of the grid. For example, the optimal value of injection of the BESS could be higher than what the energy level of the battery allows; therefore, the estimated value should be rectified to the actual value so that the simulation is as realistic as possible. The algorithm developed to represent this aspect is presented in Appendix D.
- With the optimal outputs of the controls obtained in the previous step, it is necessary to run the power flow. In this case, in order to be consistent with the previous steps in the study, the power flow utilized will be the DistFlow.
- Once the simulation is complete, the demands are updated, and the power flow is run again. This new solution is introduced in the model and the process is repeated iteratively until the operation period is completed

The process of design and testing of the controls is carried out in Matlab [19], utilizing functions from the Matpower Library [15].

3.7. Methodology Overview

This section aims to provide a graphic summary of the proposed methodology so that all steps involved and their connection can be better understood.

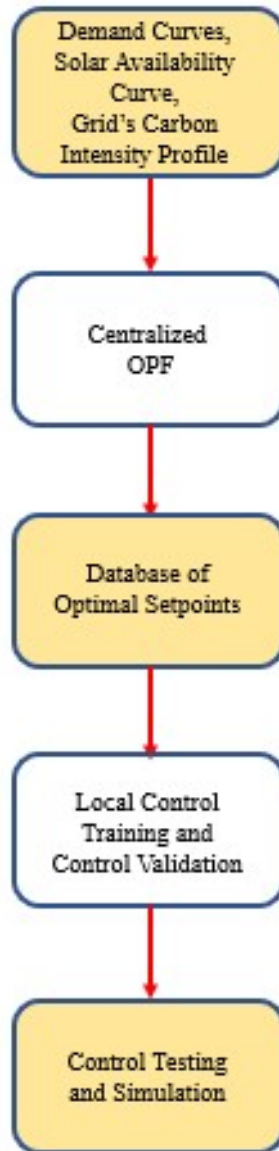


Figure 22. Methodology Overview

4. Results Analysis

The objective of this section is to show the results obtained with the proposed OPF for two different cases: a 4-bus base case and a 18-bus case. Both cases have been obtained from the Matpower library [15].

4.1. Base case: 4-bus grid

The aim of starting the analysis with a simple 4-bus network is to first test the algorithm in a less complex environment so that transcendental issues can be identified and solved. The structure of the grid in study is the following:

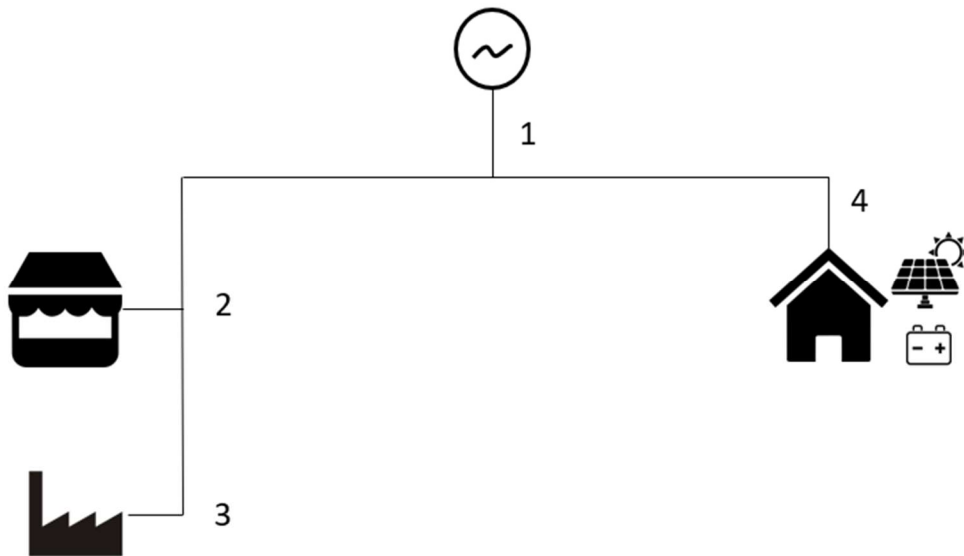


Figure 23. 4-bus Grid schematic

The bus 4 is the only one with DG units in this network. Bus 1 represents the connection to the bulk system and is treated as the slack; the other two buses, 2 and 3, are load buses with no generation capabilities. For the case's parameters refer to Appendix B.

First, the OPF is run for the grid without BESS. The purpose of this initial solving step is to provide an emissions reference for the grid, so that the impact of the introduction of the BESS can be analyzed:

- Carbon Footprint without BESS: 7885 kg CO₂

The above presented result corresponds to the 3-day operation of the 4-bus grid without energy storage capability. This serves as a benchmark to carry out an assessment of the enhancement produced by the introduction of the batteries, as well as an evaluation of the marginal economic cost of the reduction of the network's carbon footprint.

4.1.1. OPF Results

This subsection analyzes the performance of the OPF when the BESS are introduced. The introduction of these systems has an impact on the variables of the network. Moreover, the carbon intensity of the grid is reduced by the action of the batteries, that harness the difference in the CO₂ intensity of the grid to optimally charge and discharge.

- Carbon Footprint with BESS: 7816 kg CO₂

The introduction of the batteries yields a carbon footprint reduction of 69 kg CO₂ during the period of operation, which corresponds to three days.

Moving on to the specific performance of the OPF, the voltages are the first variables to be analyzed:

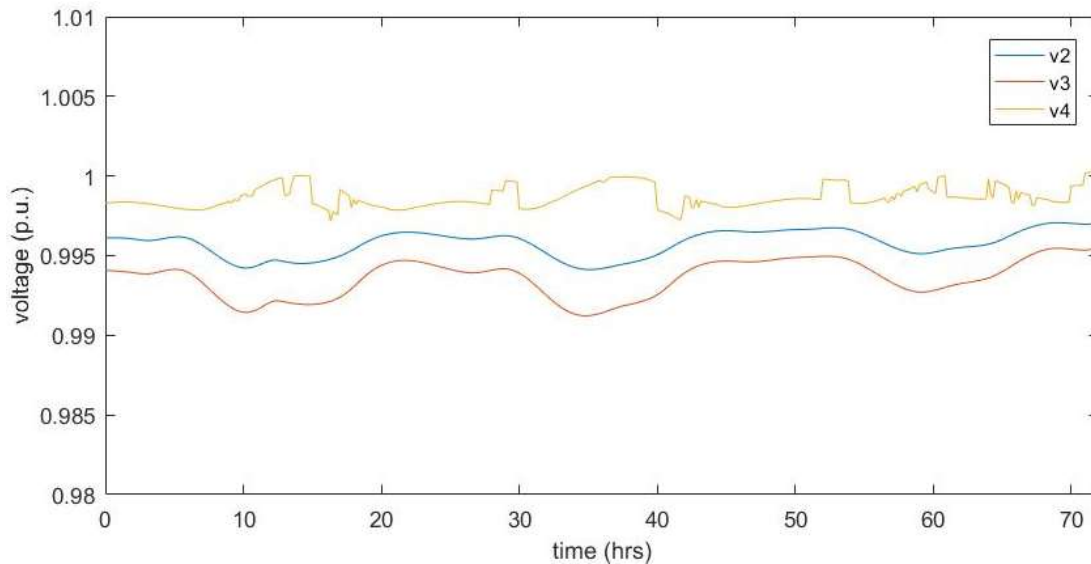


Figure 24. 4-bus Grid, OPF Voltage Response

The voltage profiles above presented correspond to the three buses with demand in the network. The three of them stay within limits during the whole period of operation. Its variation is very low, which is a consequence of the low impedance value of the lines. Moreover, it can be clearly identified the buses that have DG and the buses that do not. Sudden changes in injection are typical of PV units and have their impact on voltage. This is the case of bus 4, which shows abrupt changes in its voltage. On the other hand, buses 2 and 3 show voltages with continuous derivatives, which is an indicator of a steadier injection.

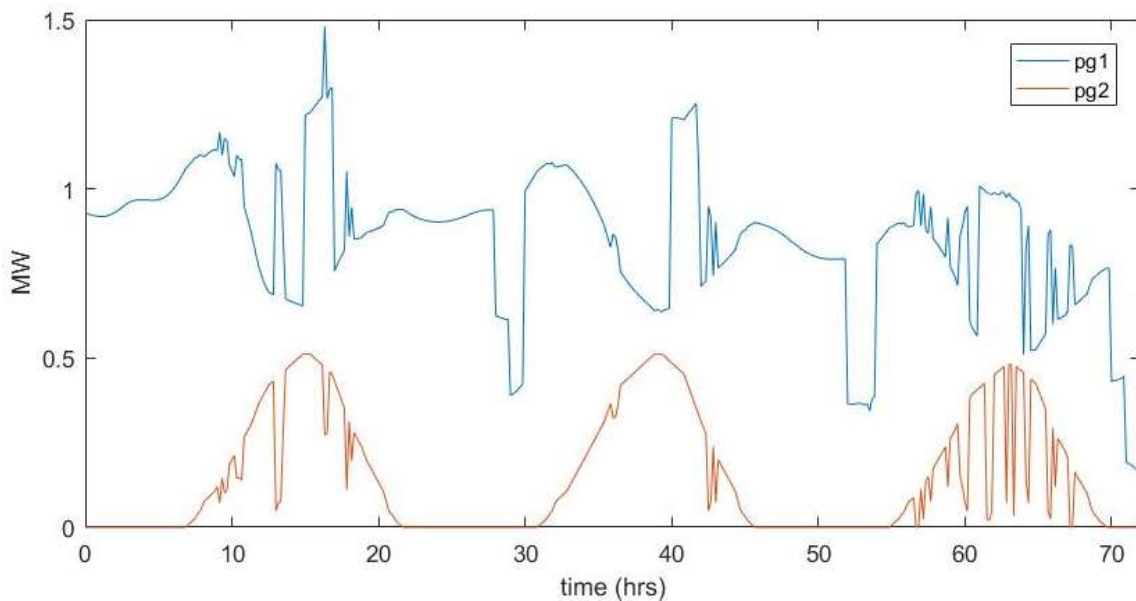


Figure 25. 4-bus Grid, OPF Generations

Above presented is the generation variation of the two generators of the grid. Generator 1 corresponds to the slack, while generator 2 refers to the PV units installed in bus 4. The DG in bus 4 follows the solar radiation curve, offering power only during the day with steep drops in generation due to cloud coverage. This has an effect on generator 1, which mirrors the variation of the PV generation. However, there are drops and peaks in the generation of the slack which do not have their equivalent in the DG generation. Those correspond to the action of the BESS.

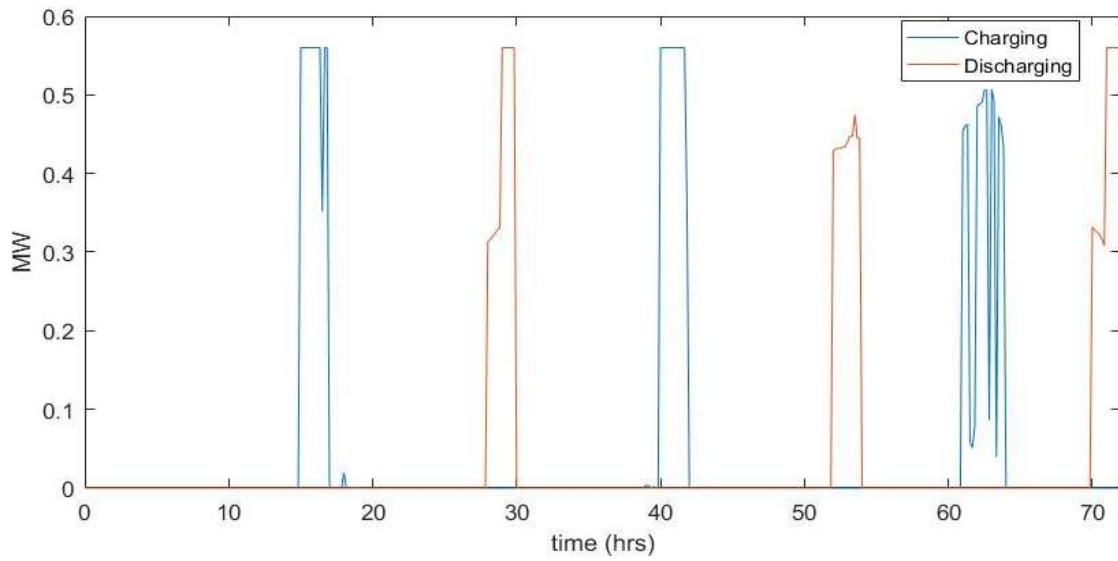


Figure 26. 4-bus Grid, BESS Charging and Discharging

Figure 16 explains the generation fluctuations in the slack in Figure 15. While the charging of the battery occurs during the afternoon, the discharging is performed right after midnight for the first two days and just before midnight for the last day. It is worth noting that this premature discharge of the battery during the last day of operation is caused by the limitation of days. Comparing with the other two days, it can be inferred the third discharge of the battery would be more optimal if the operation time were to be lengthened.

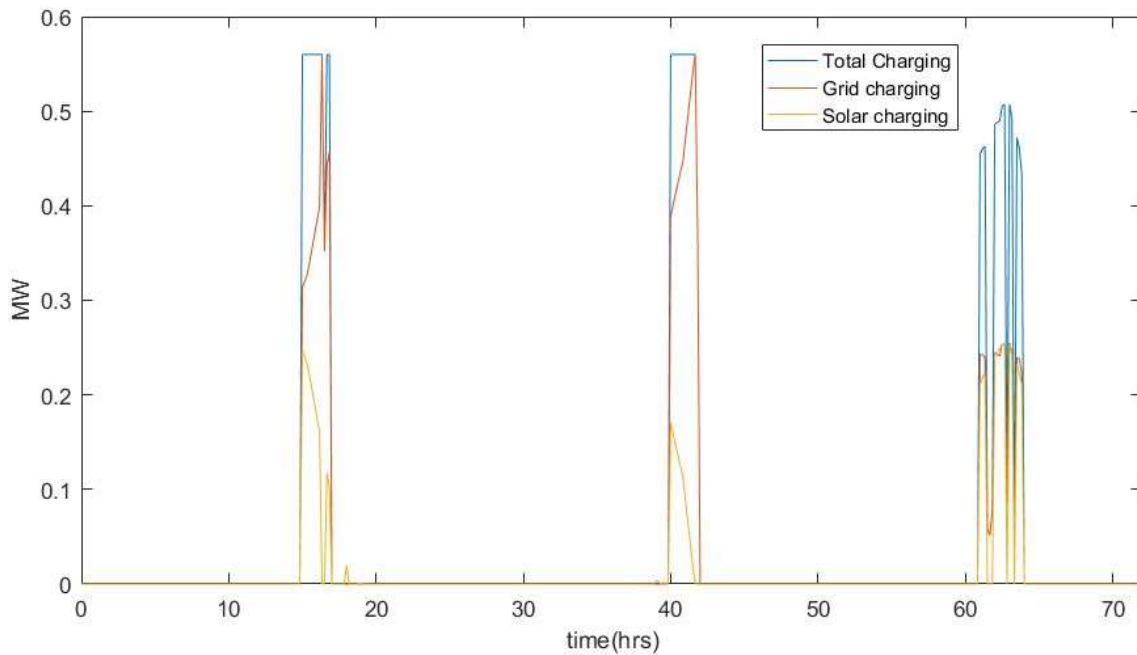


Figure 27. 4-bus Grid, BESS Charging Source

Moreover, the charging can be divided in two different variables depending on the source of the power: grid charging and solar charging. This way, it is possible to evaluate the importance of each of the sources in the performance of the battery. It is worth noting that, during the first two days, the majority of the power is provided by the grid, while during the last day, the relevance of the two sources is equal. Furthermore, it can be inferred that, although in terms of magnitude the contribution of solar is lower, the solar availability clearly influences the power drawn from the grid, dictating the path towards optimality.

The previous two graphs capture the behavior of the BESS from a power point of view, which can now be translated in order to analyze the performance of the battery from an energy perspective. This analysis is carried out by contemplating the level of discharge of the BESS, since a key aspect of the batteries installed is the requirement of a minimum level of energy at any time of operation. Specifically, the DoD of these units is 96% of their available energy.

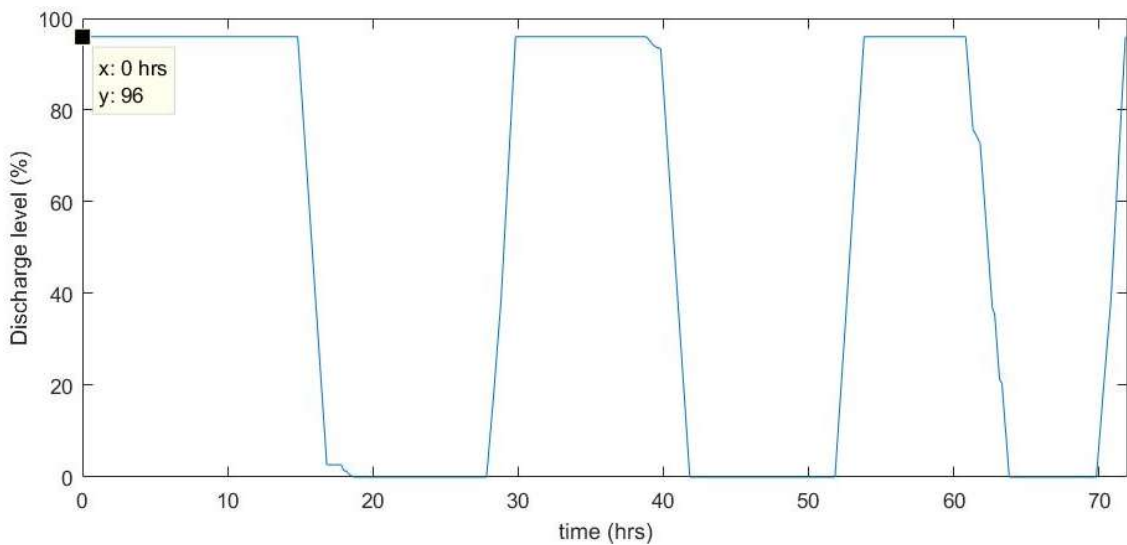


Figure 28. 4-bus Grid, BESS Discharge Level

The charge of the battery evolves from an initial condition of full discharge to a final equivalent condition that ensures the solution is actually optimal. The power sequence already explained yields an evolution of the energy in the battery that varies between fully charged and the DoD specification. As well as in the power graph, the energetic behavior during the last day suggests that the battery has been discharged sooner than what would be fully optimal if the operation time were to be lengthened.

This initial assessment is useful to provide a general glimpse of the performance of the power flow. However, this case is not ideal to carry out the design of the local controls. The reason can be found in Figure 14: the range of variation of the voltages is not wide

Moreover, this value allows an economic evaluation of the marginal cost of the introduction of the batteries.

4.2.1. OPF results

This subsection aims to analyze the performance of the centralized OPF in the grid. First, the main indicator to analyze is the carbon footprint of the new solution, so that it can be compared to the case without batteries:

- Carbon Footprint with BESS: 72613 kg CO₂

Furthermore, this section tries to verify the new data does not present the limitations of the previous case's results, and that it is adequate to perform the second task of the study: the design of the local controls.

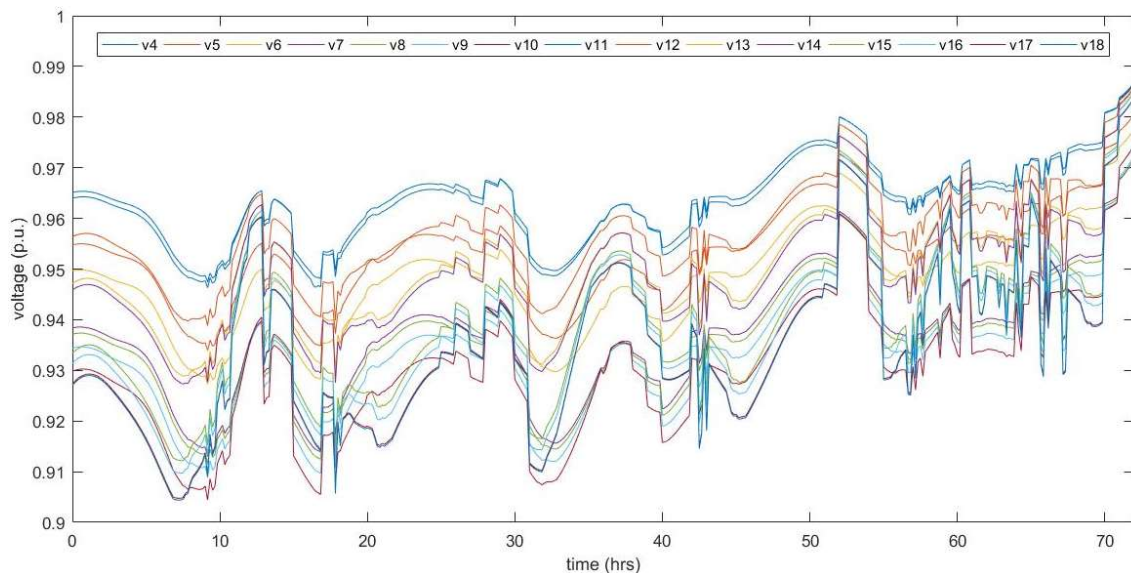


Figure 30. 18-bus Grid, OPF Voltage response

Figure 20 shows the range of variation of the voltages has increased significantly compared to the base case. The new data seems more robust in order to carry out a data driven control design. Regarding the performance, the voltage profiles present similarities with the profile obtained in the previous case for the bus with PV units. The sudden fluctuations in the voltage's magnitude are caused by the action of the BESS, either charging or discharging. Moreover, it is worth noting all voltages seem to evolve together, which suggests their BESS behave in a similar way.

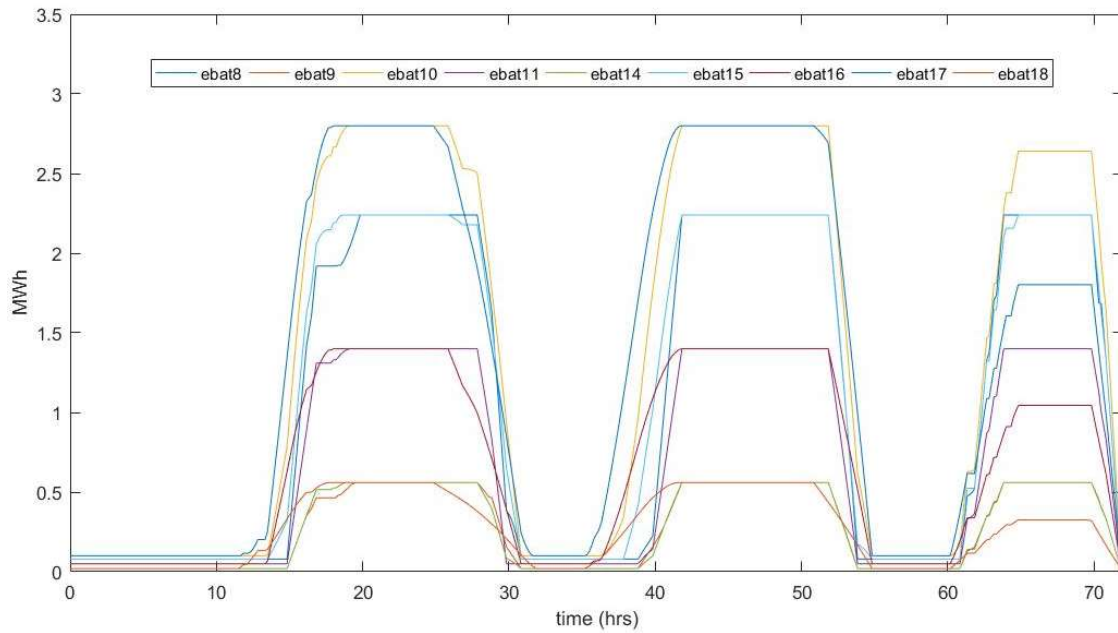


Figure 31. 18-bus Grid, OPF BESS energy

As shown in Figure 21, the BESS installed in the different buses are indeed following similar trends, which show differences based on the energy and power specifications, which are different depending on the size of the consumers. Similar to the base case, the energy level during the last day of operation suggests the optimal dispatch is constrained by the limitation of days, causing a premature charge and discharge of the batteries during the third day.

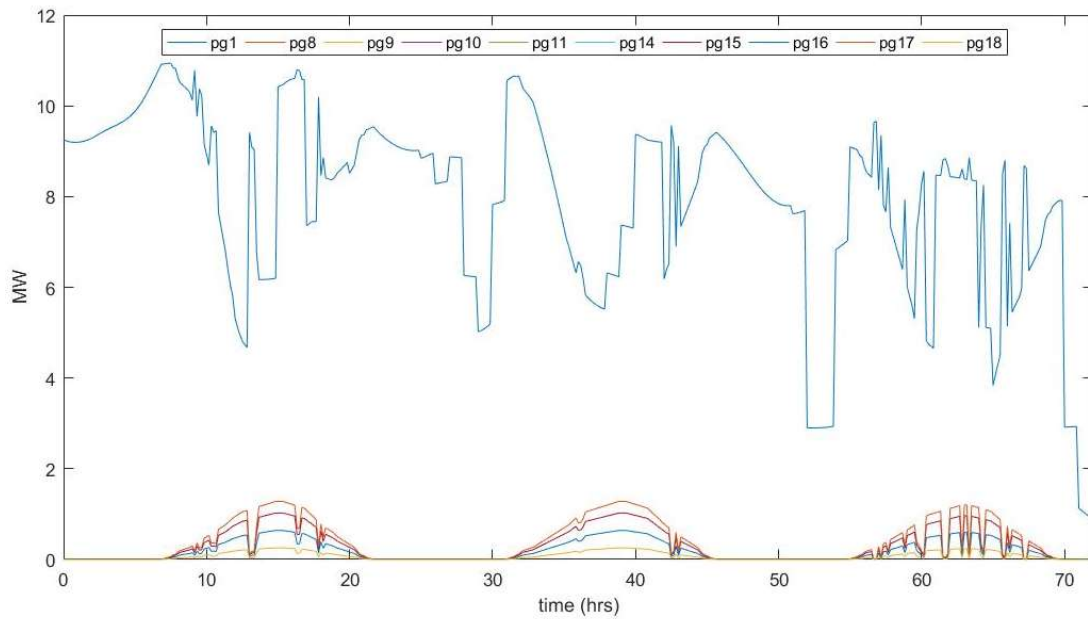


Figure 32. 18-bus Grid, OPF Generations

The action of the BESS is shown as well in the graph above. The deep valleys in the generation of the slack, which occur during the beginning of the second and the third day and the end of the period of operation, correspond to the discharge of the batteries during that same interval of time. Moreover, the continuous variation in solar radiation forces the slack to modify its generation accordingly. This last assessment remarks the importance of having flexible sources of energy that can ensure the reliability of the system. In order to respond to the sudden changes in generation and demand in the network caused by PV units and BESS, it is paramount to support the network with a main grid that can decrease or increase its generation when needed.

4.2.2. Control Design

The second part of the study aims to design local controls for the bus voltage. Local controls utilize measurements performed in a certain node to control its voltage independently of the rest of the grid. Therefore, it is key to decide which are the explanatory variables and which is the dependent variable. The dependent variable is the command introduced in the controller; therefore, it must be a variable that can be directly changed.

By analyzing the data obtained in the previous step, it can be inferred that no curtailment of solar power is needed for the given operating conditions. Thus, the solar generation is continuously maximized and does not make sense to build the control on the DG generation. For the purpose of this study, the BESS injection has been chosen as the dependent variable rather than the generation of the PV units. The injection variable of the batteries becomes positive when discharging and negative when charging.

Once the dependent variable has been chosen, it is necessary to decide the explanatory variables. Among this group of variables, bus voltage has to be included since the purpose is to control it. The process of deciding which are to be included in the model was carried out by including several possible bus measurements and ruling out those with no explanatory potential. The set of potential explanatory variables was the following: bus voltage, bus demand, PV bus generation and battery energy level. After running several tests, the structure of the final model was the following:

- Dependent variable: BESS injection.
- Explanatory variables: PV bus generation (linear and quadratic components), bus demand (linear component), battery energy level (linear component) and bus voltage (quadratic component).

The coefficient's analysis for the controls of the different buses is presented below:

BUS	COEFFICIENT ANALYSIS																																			
8	<p>Linear regression model: battery_var_8 ~ 1 + pd8 + pg8 + dod8 + pg8_2 + v8_2</p> <p>Estimated Coefficients:</p> <table border="1" style="width: 100%; border-collapse: collapse;"> <thead> <tr> <th></th> <th style="text-align: center;">Estimate</th> <th style="text-align: center;">SE</th> <th style="text-align: center;">tStat</th> <th style="text-align: center;">pValue</th> </tr> </thead> <tbody> <tr> <td>(Intercept)</td> <td style="text-align: center;">-13</td> <td style="text-align: center;">0.89159</td> <td style="text-align: center;">-14.581</td> <td style="text-align: center;">2.3665e-39</td> </tr> <tr> <td>pd8</td> <td style="text-align: center;">1.3524</td> <td style="text-align: center;">0.19915</td> <td style="text-align: center;">6.7907</td> <td style="text-align: center;">3.7626e-11</td> </tr> <tr> <td>pg8</td> <td style="text-align: center;">0.24669</td> <td style="text-align: center;">0.15355</td> <td style="text-align: center;">1.6066</td> <td style="text-align: center;">0.10887</td> </tr> <tr> <td>dod8</td> <td style="text-align: center;">0.0047155</td> <td style="text-align: center;">0.00039902</td> <td style="text-align: center;">11.818</td> <td style="text-align: center;">4.5521e-28</td> </tr> <tr> <td>pg8_2</td> <td style="text-align: center;">-0.76448</td> <td style="text-align: center;">0.16273</td> <td style="text-align: center;">-4.6978</td> <td style="text-align: center;">3.5542e-06</td> </tr> <tr> <td>v8_2</td> <td style="text-align: center;">13.752</td> <td style="text-align: center;">0.90567</td> <td style="text-align: center;">15.184</td> <td style="text-align: center;">6.2652e-42</td> </tr> </tbody> </table> <p>Number of observations: 432, Error degrees of freedom: 426 Root Mean Squared Error: 0.279 R-squared: 0.567, Adjusted R-Squared 0.562 F-statistic vs. constant model: 112, p-value = 3.78e-75</p> <ul style="list-style-type: none"> - R-Squared could be considered low. - Pvalue of the generation coefficient is high. The linear component of the generation could be removed. 		Estimate	SE	tStat	pValue	(Intercept)	-13	0.89159	-14.581	2.3665e-39	pd8	1.3524	0.19915	6.7907	3.7626e-11	pg8	0.24669	0.15355	1.6066	0.10887	dod8	0.0047155	0.00039902	11.818	4.5521e-28	pg8_2	-0.76448	0.16273	-4.6978	3.5542e-06	v8_2	13.752	0.90567	15.184	6.2652e-42
	Estimate	SE	tStat	pValue																																
(Intercept)	-13	0.89159	-14.581	2.3665e-39																																
pd8	1.3524	0.19915	6.7907	3.7626e-11																																
pg8	0.24669	0.15355	1.6066	0.10887																																
dod8	0.0047155	0.00039902	11.818	4.5521e-28																																
pg8_2	-0.76448	0.16273	-4.6978	3.5542e-06																																
v8_2	13.752	0.90567	15.184	6.2652e-42																																
9	<p>Linear regression model: battery_var_9 ~ 1 + pd9 + pg9 + dod9 + pg9_2 + v9_2</p> <p>Estimated Coefficients:</p> <table border="1" style="width: 100%; border-collapse: collapse;"> <thead> <tr> <th></th> <th style="text-align: center;">Estimate</th> <th style="text-align: center;">SE</th> <th style="text-align: center;">tStat</th> <th style="text-align: center;">pValue</th> </tr> </thead> <tbody> <tr> <td>(Intercept)</td> <td style="text-align: center;">-3.2348</td> <td style="text-align: center;">0.19058</td> <td style="text-align: center;">-16.973</td> <td style="text-align: center;">9.9535e-50</td> </tr> <tr> <td>pd9</td> <td style="text-align: center;">1.5583</td> <td style="text-align: center;">0.18193</td> <td style="text-align: center;">8.5655</td> <td style="text-align: center;">1.988e-16</td> </tr> <tr> <td>pg9</td> <td style="text-align: center;">0.19724</td> <td style="text-align: center;">0.13665</td> <td style="text-align: center;">1.4434</td> <td style="text-align: center;">0.14964</td> </tr> <tr> <td>dod9</td> <td style="text-align: center;">0.0011512</td> <td style="text-align: center;">8.8238e-05</td> <td style="text-align: center;">13.047</td> <td style="text-align: center;">5.7459e-33</td> </tr> <tr> <td>pg9_2</td> <td style="text-align: center;">-2.9132</td> <td style="text-align: center;">0.58295</td> <td style="text-align: center;">-4.9973</td> <td style="text-align: center;">8.503e-07</td> </tr> <tr> <td>v9_2</td> <td style="text-align: center;">3.4059</td> <td style="text-align: center;">0.19293</td> <td style="text-align: center;">17.653</td> <td style="text-align: center;">9.7168e-53</td> </tr> </tbody> </table> <p>Number of observations: 432, Error degrees of freedom: 426 Root Mean Squared Error: 0.0628 R-squared: 0.627, Adjusted R-Squared 0.622 F-statistic vs. constant model: 143, p-value = 7.57e-89</p> <ul style="list-style-type: none"> - R-squared could be considered low. - Pvalue of the generation coefficient is high. The linear component of the generation could be removed. 		Estimate	SE	tStat	pValue	(Intercept)	-3.2348	0.19058	-16.973	9.9535e-50	pd9	1.5583	0.18193	8.5655	1.988e-16	pg9	0.19724	0.13665	1.4434	0.14964	dod9	0.0011512	8.8238e-05	13.047	5.7459e-33	pg9_2	-2.9132	0.58295	-4.9973	8.503e-07	v9_2	3.4059	0.19293	17.653	9.7168e-53
	Estimate	SE	tStat	pValue																																
(Intercept)	-3.2348	0.19058	-16.973	9.9535e-50																																
pd9	1.5583	0.18193	8.5655	1.988e-16																																
pg9	0.19724	0.13665	1.4434	0.14964																																
dod9	0.0011512	8.8238e-05	13.047	5.7459e-33																																
pg9_2	-2.9132	0.58295	-4.9973	8.503e-07																																
v9_2	3.4059	0.19293	17.653	9.7168e-53																																

10	<p>Linear regression model: battery_var_10 ~ 1 + pd10 + pg10 + dod10 + pg10_2 + v10_2</p> <p>Estimated Coefficients:</p> <table border="1"> <thead> <tr> <th></th> <th>Estimate</th> <th>SE</th> <th>tStat</th> <th>pValue</th> </tr> </thead> <tbody> <tr> <td>(Intercept)</td> <td>-12.53</td> <td>0.55319</td> <td>-22.65</td> <td>4.008e-75</td> </tr> <tr> <td>pd10</td> <td>1.5531</td> <td>0.12025</td> <td>12.916</td> <td>1.9576e-32</td> </tr> <tr> <td>pg10</td> <td>0.18862</td> <td>0.086196</td> <td>2.1883</td> <td>0.029191</td> </tr> <tr> <td>dod10</td> <td>0.0041905</td> <td>0.00028433</td> <td>14.739</td> <td>5.0569e-40</td> </tr> <tr> <td>pg10_2</td> <td>-0.62803</td> <td>0.074429</td> <td>-8.438</td> <td>5.0864e-16</td> </tr> <tr> <td>v10_2</td> <td>13.061</td> <td>0.55404</td> <td>23.574</td> <td>3.0034e-79</td> </tr> </tbody> </table> <p>Number of observations: 432, Error degrees of freedom: 426 Root Mean Squared Error: 0.2 R-squared: 0.791, Adjusted R-Squared 0.788 F-statistic vs. constant model: 322, p-value = 3.79e-142</p> <ul style="list-style-type: none"> - R-squared value is reasonable. - All coefficients are acceptable at a 5% significance. 		Estimate	SE	tStat	pValue	(Intercept)	-12.53	0.55319	-22.65	4.008e-75	pd10	1.5531	0.12025	12.916	1.9576e-32	pg10	0.18862	0.086196	2.1883	0.029191	dod10	0.0041905	0.00028433	14.739	5.0569e-40	pg10_2	-0.62803	0.074429	-8.438	5.0864e-16	v10_2	13.061	0.55404	23.574	3.0034e-79
	Estimate	SE	tStat	pValue																																
(Intercept)	-12.53	0.55319	-22.65	4.008e-75																																
pd10	1.5531	0.12025	12.916	1.9576e-32																																
pg10	0.18862	0.086196	2.1883	0.029191																																
dod10	0.0041905	0.00028433	14.739	5.0569e-40																																
pg10_2	-0.62803	0.074429	-8.438	5.0864e-16																																
v10_2	13.061	0.55404	23.574	3.0034e-79																																
11	<p>Linear regression model: battery_var_11 ~ 1 + pd11 + pg11 + dod11 + pg11_2 + v11_2</p> <p>Estimated Coefficients:</p> <table border="1"> <thead> <tr> <th></th> <th>Estimate</th> <th>SE</th> <th>tStat</th> <th>pValue</th> </tr> </thead> <tbody> <tr> <td>(Intercept)</td> <td>-12.603</td> <td>0.84292</td> <td>-14.952</td> <td>6.2344e-41</td> </tr> <tr> <td>pd11</td> <td>1.6027</td> <td>0.21129</td> <td>7.5856</td> <td>2.098e-13</td> </tr> <tr> <td>pg11</td> <td>0.32049</td> <td>0.15699</td> <td>2.0415</td> <td>0.04182</td> </tr> <tr> <td>dod11</td> <td>0.0029133</td> <td>0.00025046</td> <td>11.632</td> <td>2.387e-27</td> </tr> <tr> <td>pg11_2</td> <td>-1.3237</td> <td>0.26567</td> <td>-4.9824</td> <td>9.1486e-07</td> </tr> <tr> <td>v11_2</td> <td>12.845</td> <td>0.83758</td> <td>15.336</td> <td>1.3964e-42</td> </tr> </tbody> </table> <p>Number of observations: 432, Error degrees of freedom: 426 Root Mean Squared Error: 0.178 R-squared: 0.566, Adjusted R-Squared 0.561 F-statistic vs. constant model: 111, p-value = 5.65e-75</p> <ul style="list-style-type: none"> - R-squared could be considered low. - All coefficients are acceptable at a 5% significance. 		Estimate	SE	tStat	pValue	(Intercept)	-12.603	0.84292	-14.952	6.2344e-41	pd11	1.6027	0.21129	7.5856	2.098e-13	pg11	0.32049	0.15699	2.0415	0.04182	dod11	0.0029133	0.00025046	11.632	2.387e-27	pg11_2	-1.3237	0.26567	-4.9824	9.1486e-07	v11_2	12.845	0.83758	15.336	1.3964e-42
	Estimate	SE	tStat	pValue																																
(Intercept)	-12.603	0.84292	-14.952	6.2344e-41																																
pd11	1.6027	0.21129	7.5856	2.098e-13																																
pg11	0.32049	0.15699	2.0415	0.04182																																
dod11	0.0029133	0.00025046	11.632	2.387e-27																																
pg11_2	-1.3237	0.26567	-4.9824	9.1486e-07																																
v11_2	12.845	0.83758	15.336	1.3964e-42																																

14

Linear regression model:
 $\text{battery_var_14} \sim 1 + \text{pd14} + \text{pg14} + \text{dod14} + \text{pg14_2} + \text{v14_2}$

Estimated Coefficients:

	Estimate	SE	tStat	pValue
(Intercept)	-4.0659	0.18189	-22.354	8.4057e-74
pd14	2.2941	0.17574	13.054	5.3761e-33
pg14	-0.25102	0.12054	-2.0824	0.037905
dod14	0.00098358	7.2353e-05	13.594	3.2459e-35
pg14_2	-1.8451	0.52353	-3.5243	0.00047057
v14_2	4.1296	0.17874	23.104	3.7322e-77

Number of observations: 432, Error degrees of freedom: 426
 Root Mean Squared Error: 0.057
 R-squared: 0.712, Adjusted R-Squared 0.709
 F-statistic vs. constant model: 211, p-value = 7.01e-113

- R-squared value is reasonable.
- All coefficients are acceptable at a 5% significance.

15

Linear regression model:
 $\text{battery_var_15} \sim 1 + \text{pd15} + \text{pg15} + \text{dod15} + \text{pg15_2} + \text{v15_2}$

Estimated Coefficients:

	Estimate	SE	tStat	pValue
(Intercept)	-12.76	0.41041	-31.091	1.2332e-111
pd15	2.4298	0.12445	19.525	4.1919e-61
pg15	-0.35266	0.083912	-4.2027	3.2146e-05
dod15	0.003088	0.00019682	15.69	4.1219e-44
pg15_2	-0.47187	0.091016	-5.1845	3.3538e-07
v15_2	12.882	0.3988	32.301	1.3437e-116

Number of observations: 432, Error degrees of freedom: 426
 Root Mean Squared Error: 0.157
 R-squared: 0.838, Adjusted R-Squared 0.836
 F-statistic vs. constant model: 440, p-value = 1.06e-165

- R-squared value is high.
- All coefficients are acceptable at a 1% significance.

16

Linear regression model:
 battery_var_16 ~ 1 + pd16 + pg16 + dod16 + pg16_2 + v16_2

Estimated Coefficients:

	Estimate	SE	tStat	pValue
(Intercept)	-5.1941	0.16949	-30.646	8.6284e-110
pd16	1.7776	0.086369	20.582	7.5355e-66
pg16	-0.30016	0.058614	-5.121	4.6118e-07
dod16	0.0010461	9.1545e-05	11.427	1.4671e-26
pg16_2	-0.65569	0.1022	-6.416	3.729e-10
v16_2	5.2177	0.16398	31.819	1.2409e-114

Number of observations: 432, Error degrees of freedom: 426
 Root Mean Squared Error: 0.0675
 R-squared: 0.876, Adjusted R-Squared 0.874
 F-statistic vs. constant model: 601, p-value = 1.79e-190

- R-squared value is high.
- All coefficients are acceptable at a 1% significance.

17

Linear regression model:
 battery_var_17 ~ 1 + pd17 + pg17 + dod17 + pg17_2 + v17_2

Estimated Coefficients:

	Estimate	SE	tStat	pValue
(Intercept)	-8.8014	0.28503	-30.879	9.3434e-111
pd17	1.6205	0.076943	21.06	5.3431e-68
pg17	-0.34576	0.052389	-6.5999	1.225e-10
dod17	0.0015977	0.00016517	9.6727	3.8772e-20
pg17_2	-0.27213	0.045673	-5.9583	5.3432e-09
v17_2	8.8445	0.27515	32.144	5.829e-116

Number of observations: 432, Error degrees of freedom: 426
 Root Mean Squared Error: 0.12
 R-squared: 0.886, Adjusted R-Squared 0.885
 F-statistic vs. constant model: 661, p-value = 3.16e-198

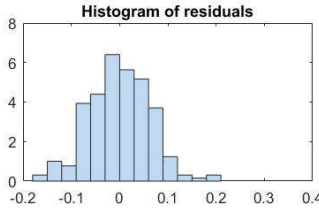
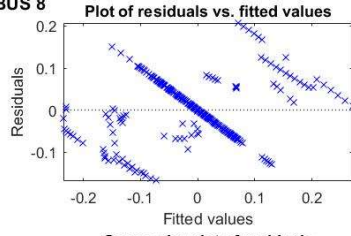
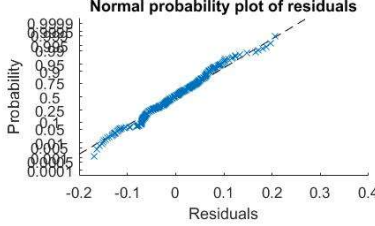
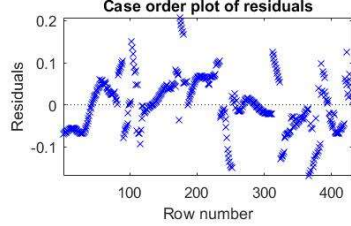
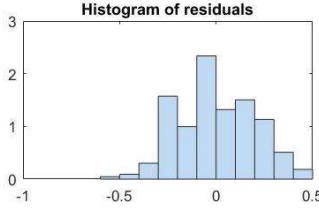
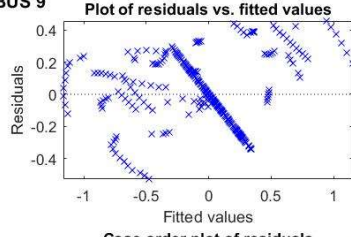
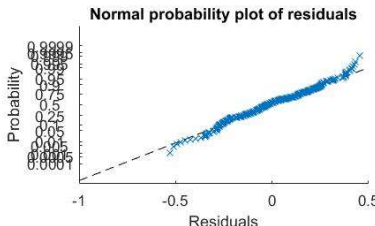
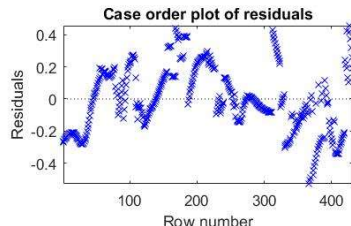
- R-squared value is high.
- All coefficients are acceptable at a 1% significance.

Linear regression model:				
battery_var_18 ~ 1 + pd18 + pg18 + dod18 + pg18_2 + v18_2				
Estimated Coefficients:				
	Estimate	SE	tStat	pValue
(Intercept)	-1.327	0.06195	-21.421	1.2867e-69
pd18	1.2614	0.084661	14.9	1.0358e-40
pg18	-0.34188	0.057929	-5.9017	7.3501e-09
dod18	0.0001768	3.7362e-05	4.7321	3.0286e-06
pg18_2	-1.2027	0.25356	-4.7433	2.8729e-06
v18_2	1.3398	0.059852	22.385	6.1506e-74
Number of observations: 432, Error degrees of freedom: 426				
Root Mean Squared Error: 0.0264				
R-squared: 0.838, Adjusted R-Squared 0.836				
F-statistic vs. constant model: 440, p-value = 8.51e-166				
<ul style="list-style-type: none"> - R-squared value is high. - All coefficients are acceptable at a 1% significance. 				

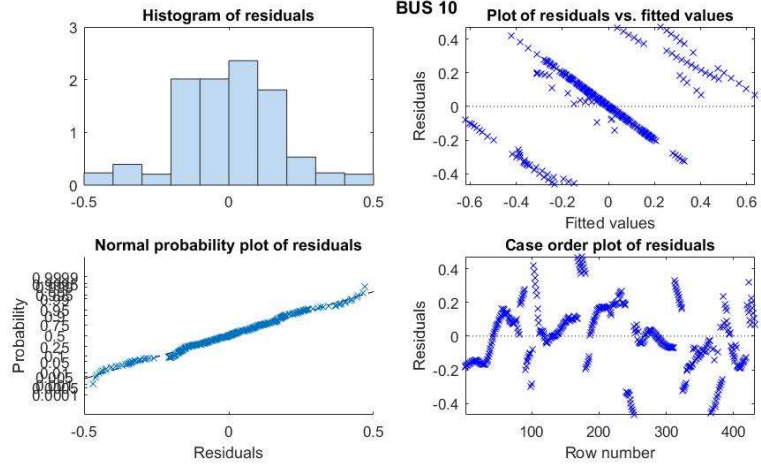
Table 3. Model Coefficients Analysis

The analysis of the coefficients yields acceptable results for all the buses. However, for buses 8 and 9, it is necessary to remove the weight associated with the linear component of the PV bus generation, since their p-values are too high to be accepted in the model.

When performing a linear regression, it is necessary to carry out a residual analysis that confirms their normality and independence. However, since the size of the data available is not large enough, the residual analysis of the obtained models is not significant. Nevertheless, the analysis is carried out anyways:

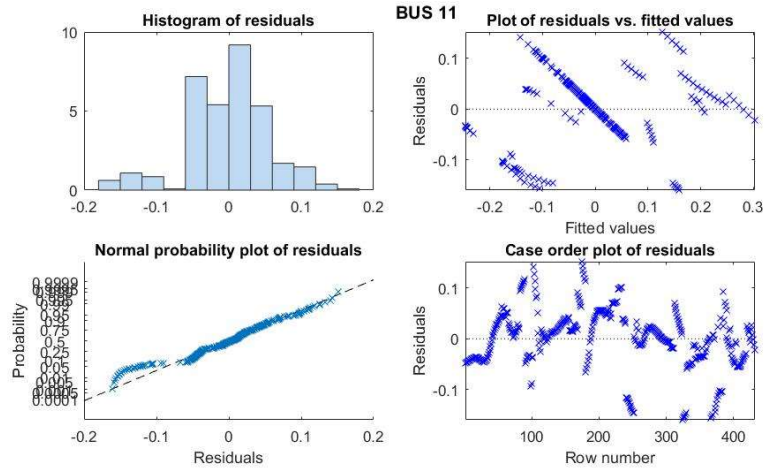
BUS	RESIDUALS ANALYSIS
8	<div style="display: flex; flex-wrap: wrap;"> <div style="width: 50%;">  <p>Histogram of residuals</p> </div> <div style="width: 50%;">  <p>BUS 8 Plot of residuals vs. fitted values</p> </div> <div style="width: 50%;">  <p>Normal probability plot of residuals</p> </div> <div style="width: 50%;">  <p>Case order plot of residuals</p> </div> </div> <ul style="list-style-type: none"> - Normality of residuals could be accepted. - Independence of residuals is denied.
9	<div style="display: flex; flex-wrap: wrap;"> <div style="width: 50%;">  <p>Histogram of residuals</p> </div> <div style="width: 50%;">  <p>BUS 9 Plot of residuals vs. fitted values</p> </div> <div style="width: 50%;">  <p>Normal probability plot of residuals</p> </div> <div style="width: 50%;">  <p>Case order plot of residuals</p> </div> </div> <ul style="list-style-type: none"> - Normality of residuals could be accepted. - Independence of residuals is denied.

10



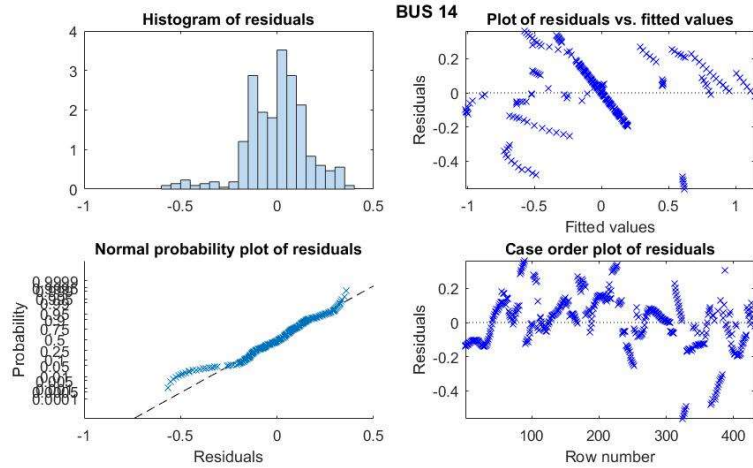
- Normality of residuals could be accepted.
- Independence of residuals is denied.

11



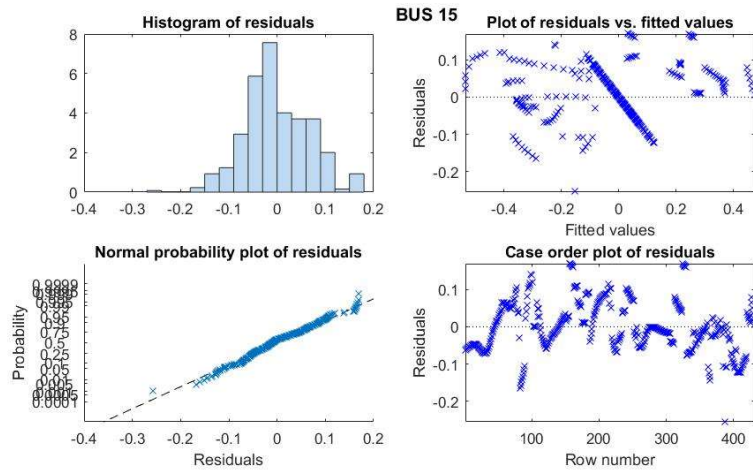
- Normality of residuals could be denied.
- Independence of residuals is denied.

14



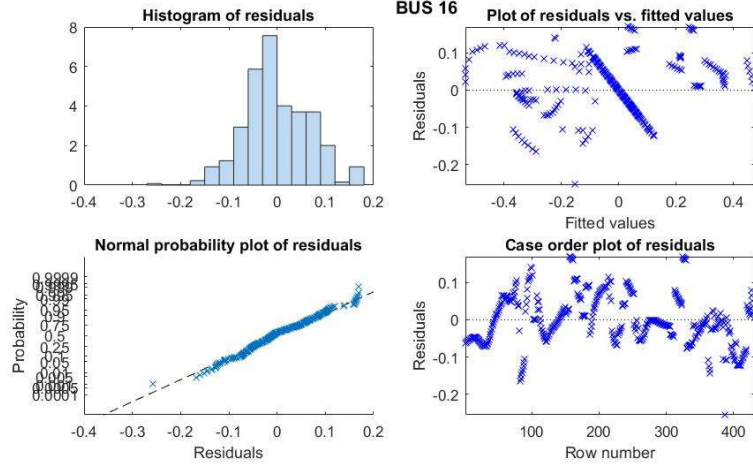
- Normality of residuals could be denied.
- Independence of residuals is denied.

15



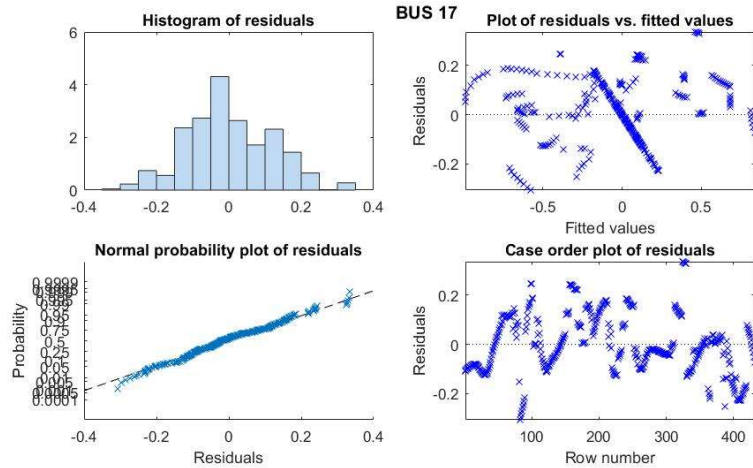
- Normality of residuals could be accepted.
- Independence of residuals is denied.

16



- Normality of residuals could be accepted.
- Independence of residuals is denied.

17



- Normality of residuals could be accepted.
- Independence of residuals is denied.

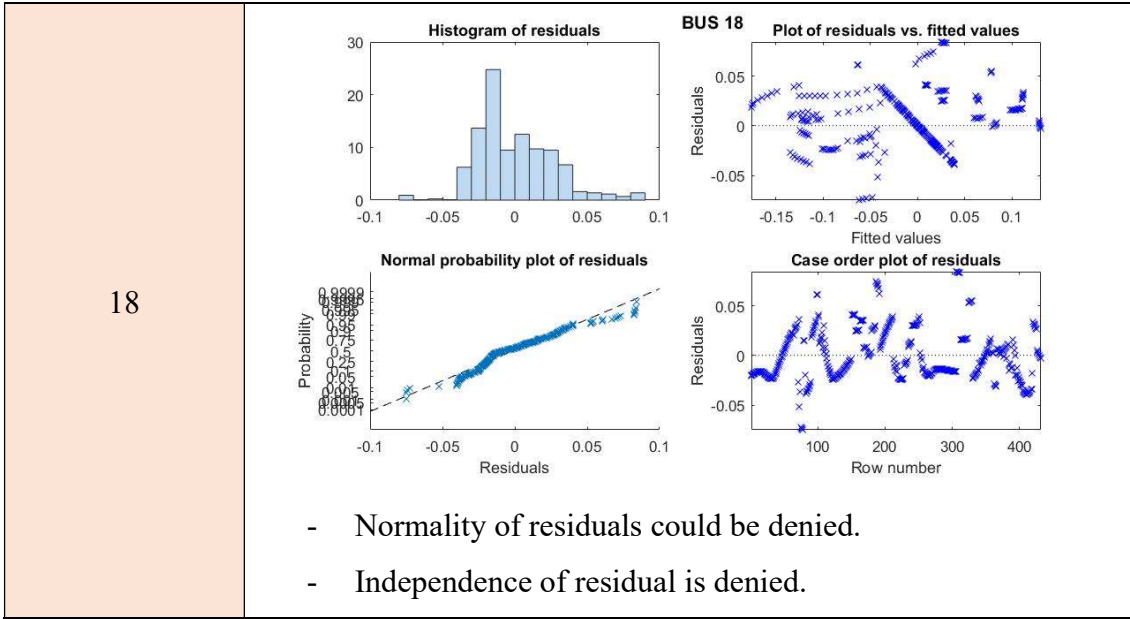


Table 4. Model Residuals Analysis

The residuals analysis reveals difficulties to accept normality and independence of residuals. However, the size of the sample is not large enough to accept the conclusions of such an analysis. It is necessary to simulate more possible operating scenarios of grid in order to obtain more observations for the different values. This way, the conclusions yielded by the residual analysis could actually be considered. Therefore, in order to test the performance of the controls, a simulation is carried out in the next section.

4.2.3. Control Testing

Once the models for all the controls have been decided, it is time to test their performance comparing it with the optimal behavior given by the solution yielded by the centralized OPF. This comparison is carried out from two different perspectives: first, comparing the voltage profiles obtained with the two different techniques; second, comparing the timely injection of the BESS with the two methods.

BUS 8

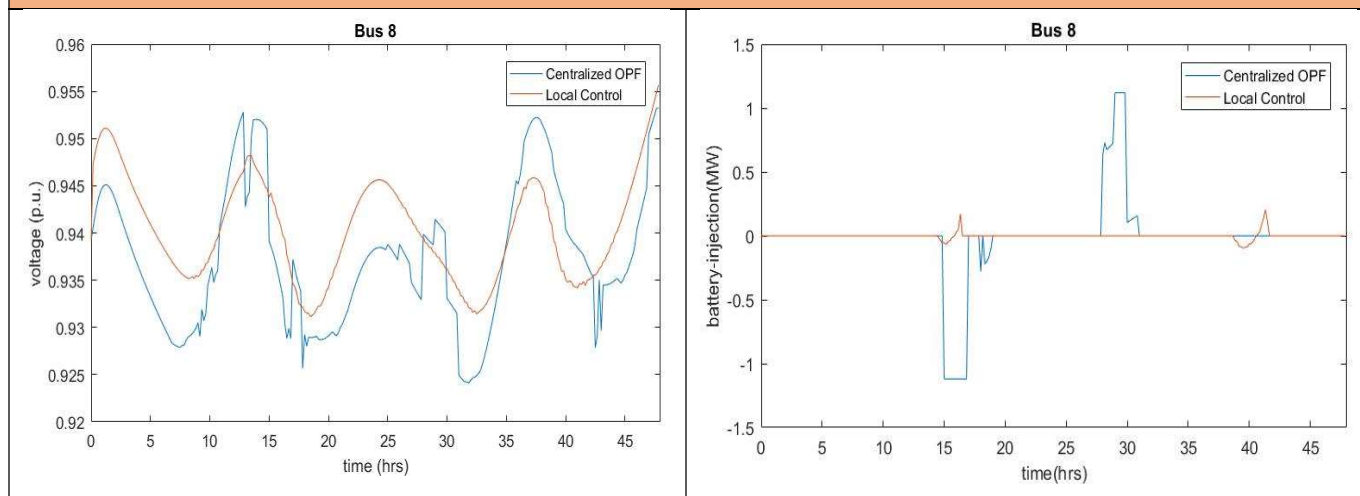


Table 5. Control Response, Bus 8

BUS 9

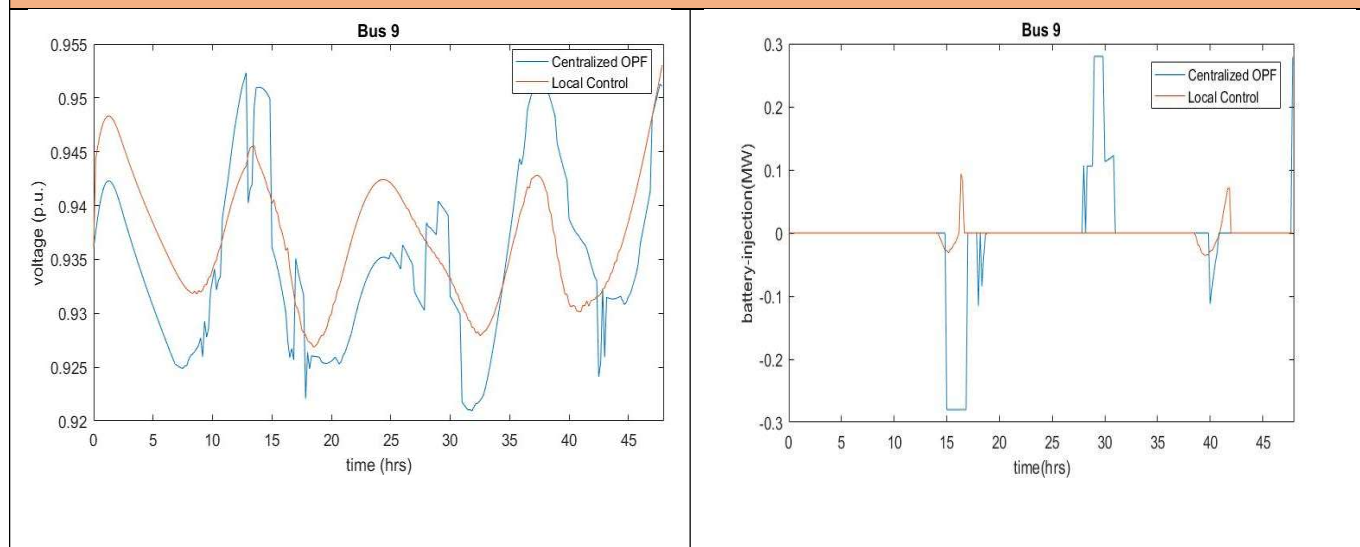


Table 6. Control Response, Bus 9

BUS 10

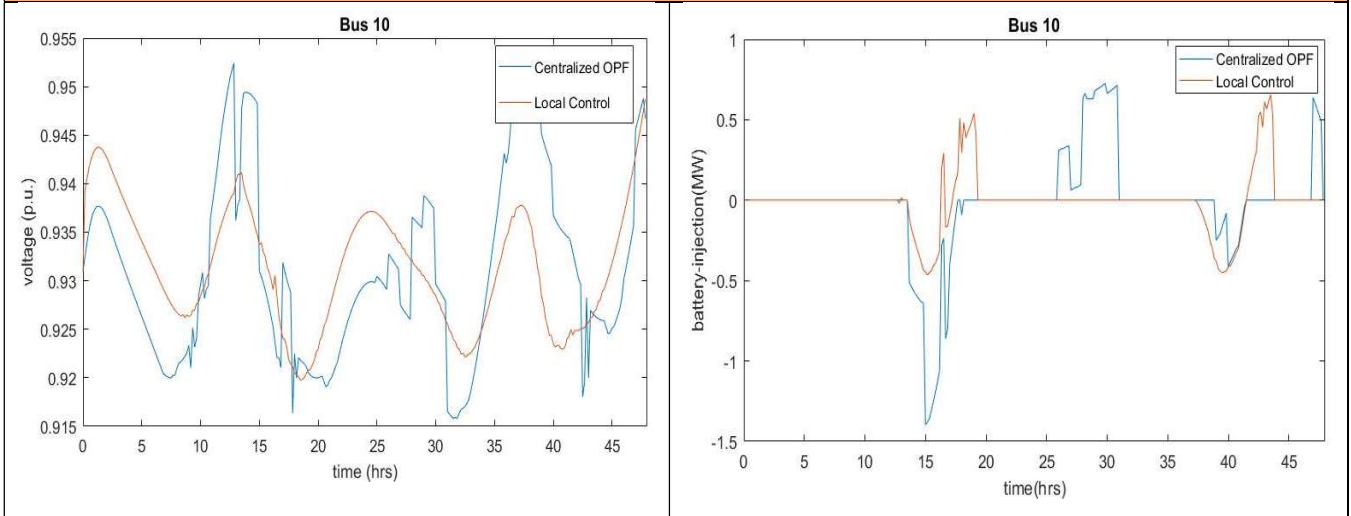


Table 7. Control Response, Bus 10

BUS 11

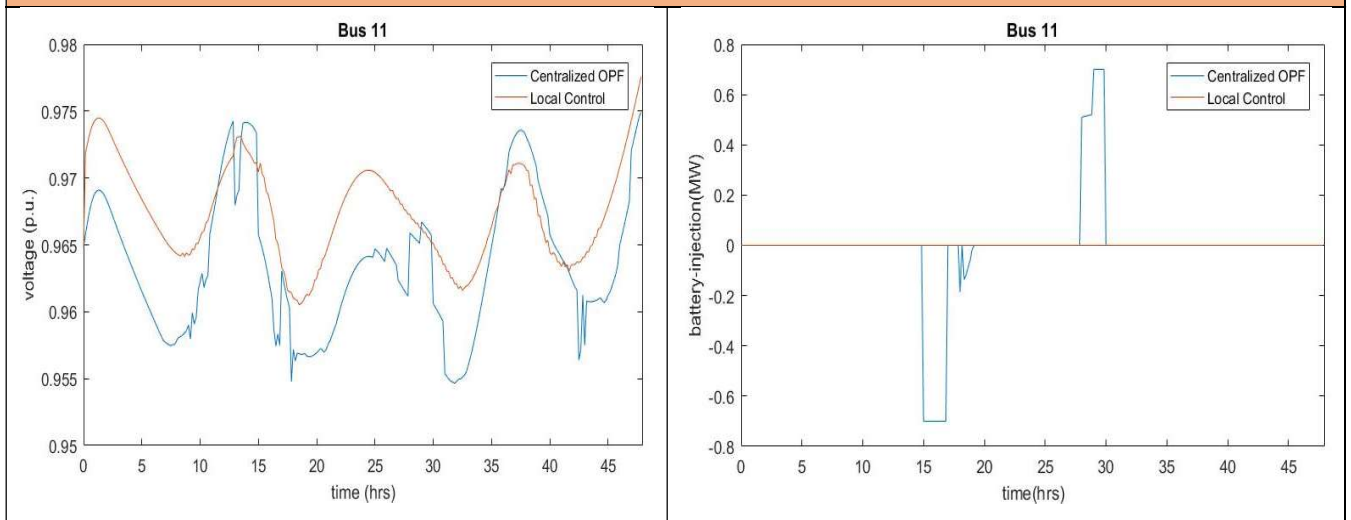


Table 8. Control Response, Bus 11

BUS 14

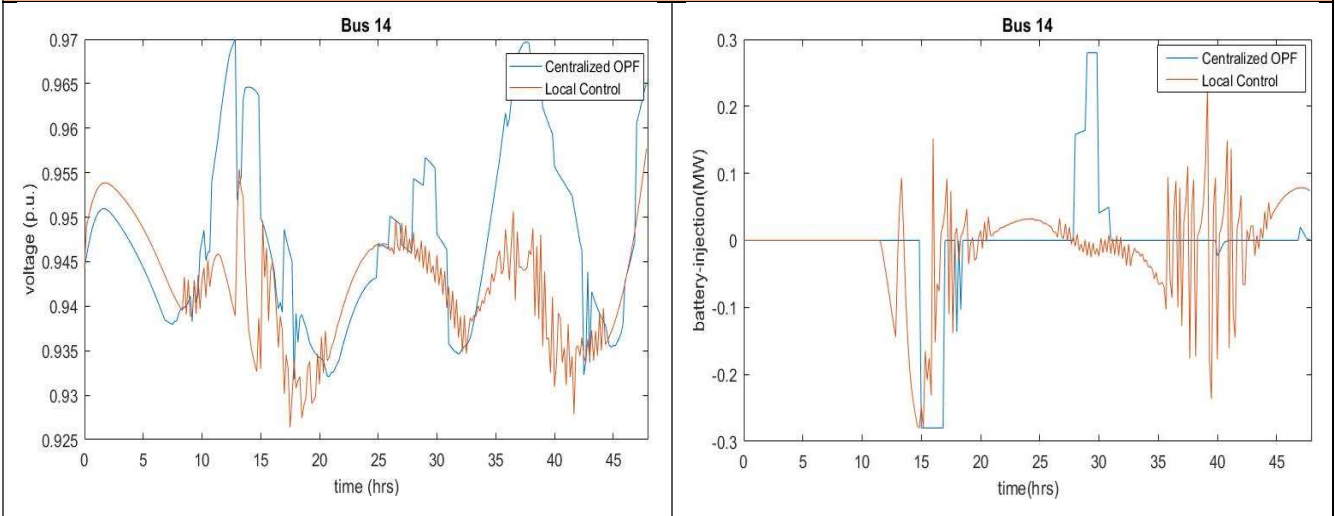


Table 9. Control Response, Bus 14

BUS 15

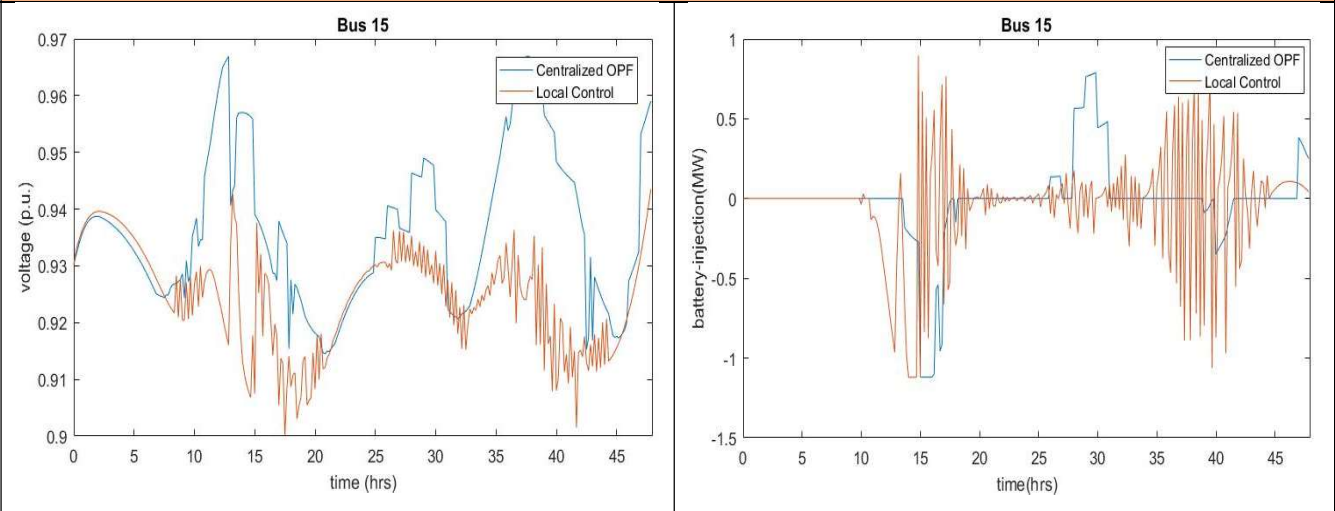


Table 10. Control Response, Bus 15

BUS 16

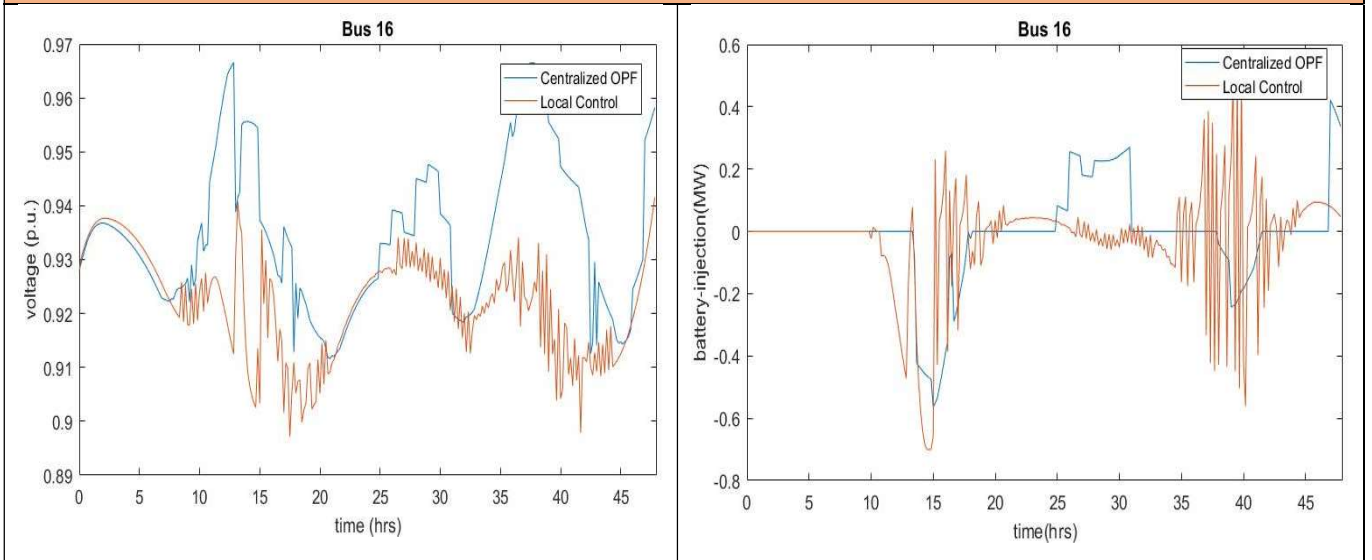


Table 11. Control Response, Bus 16

BUS 17

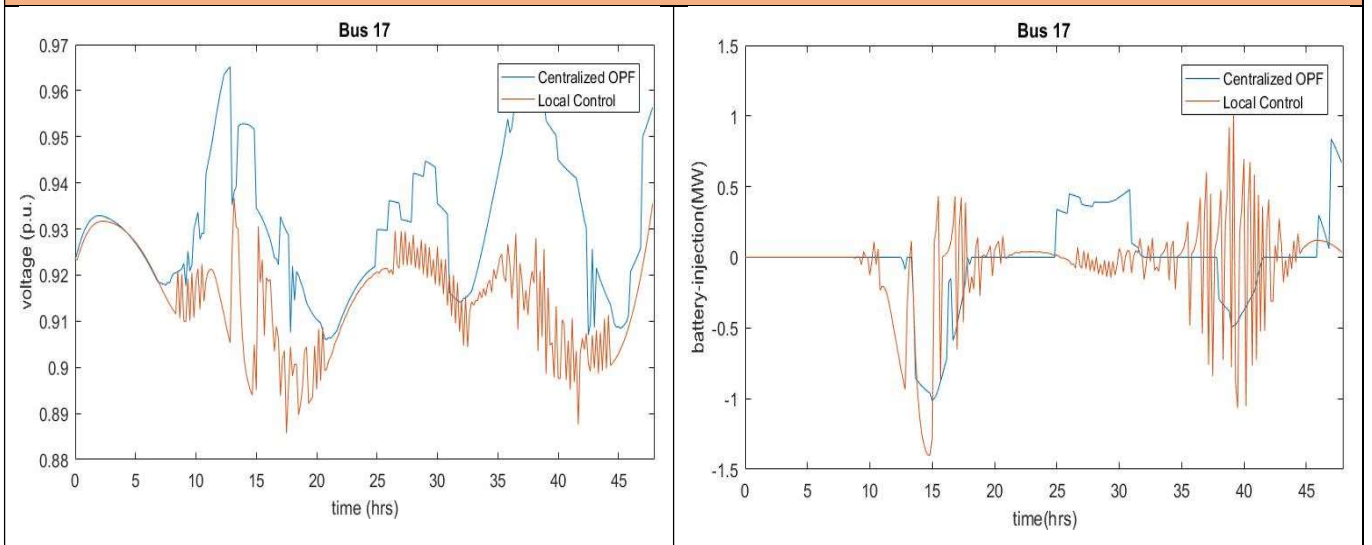


Table 12. Control Response, Bus 17

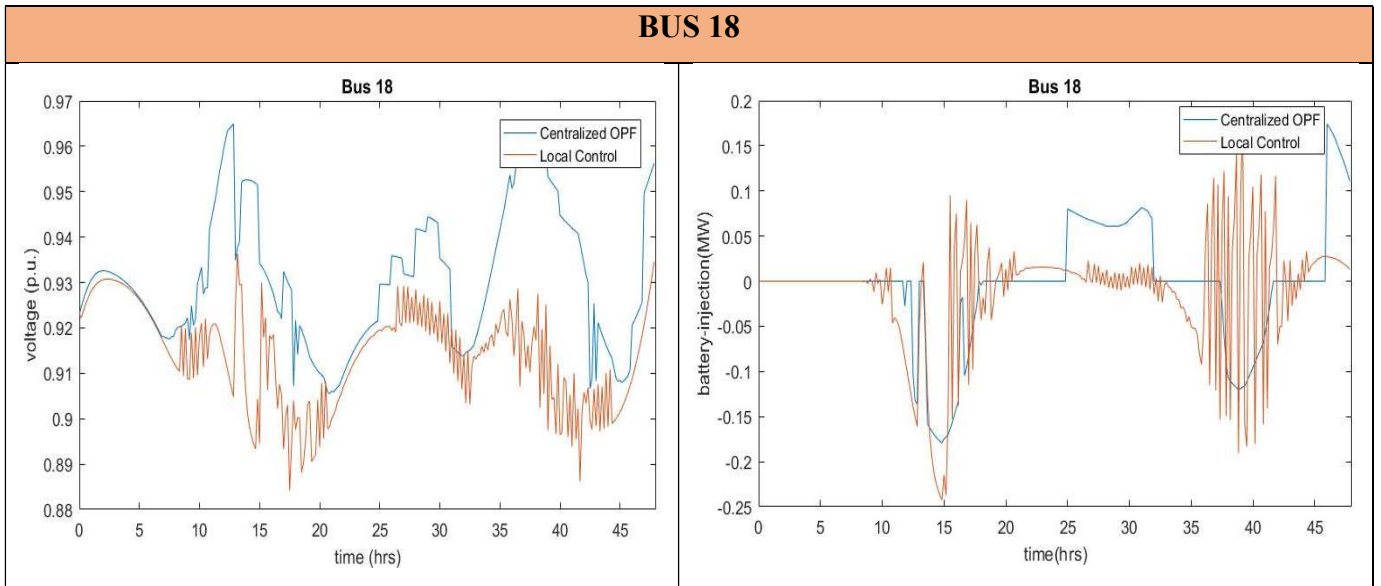


Table 13. Control Response, Bus 18

The results above presented can be divided into two different groups: the first group, formed by buses 8,9,10 and 11, shows a softer voltage response than the other group, formed by the resting buses. This differentiation seems to be determined by the location of the buses, establishing two areas within the grid with two characteristic responses. This is exemplified by the constant changes in the BESS injections of the second group, which change from charging to discharging repeatedly. This translates into deep fluctuations in the voltage profile, which suggests that clamping the response of the control could be necessary in order to soften the variation. Moreover, the controls for buses 17 and 18 should be redesigned, since the lower bound of the voltage safety range is violated.

To sum up, the design and testing of the control carried out in this study is intended to be an initial step towards obtaining a more robust data driven control. The results obtained suggest the model can be significantly enhanced by the amplification of the size of the sample and the research of other possible design techniques. Although the voltage response given by the control follows the optimal trend set by the centralized OPF, it is worth mentioning the voltage response of the second group could result in stability problems for the grid.

5. Economic and Environmental Impact Assessment

The objective of this section is to analyze the implications of the introduction of the BESS from both an economic and environmental point of view. This assessment focuses on the optimal solution provided by the OPF, which serves as benchmark of the highest CO₂ reduction potential achievable with the introduction of the batteries. This is the reason why an initial solution without the batteries was provided in the results section. Moreover, this two-face analysis has been merged into a single chapter since they are deeply correlated and, in the future, this correlation could be strengthened by the introduction of a carbon tax that enables to internalize the cost of emitting CO₂. Therefore, the ultimate objective of this section is to provide the marginal monetary cost of reducing the carbon footprint of the grid. For such purpose, both the cost of the batteries and the reduction of the CO₂ emissions are needed. This analysis will consider the optimal solution obtained for both the base case and the case study, with the purpose of studying any improvements provided by escalation.

On the one hand, the batteries selected are the Powerwall designed by Tesla. They could be obtained for \$7,500 each, with a 10-year warranty. Therefore, a 10-year linear depreciation is assumed, yielding the following unit annual cost:

Unit price (\$)	Years of warranty	Unit annual cost (\$/year)
7,500	10	750

Table 14. Battery unit price

Once the unit annual cost has been deducted, it is necessary to provide the number of batteries installed. Moreover, it is important to consider that the carbon emissions obtained are the result of a 3-day operation time; thus, this number must be scaled to an annual framework. Therefore, for the two different cases, the following results are obtained:

CASE	Emissions without BESS in 3-day period (kg CO₂e)	Emissions with BESS in 3-day period (kg CO₂e)	Annual reduction of emissions (kg CO₂e)	N° of batteries installed	Total annual cost of the batteries (\$)	Marginal cost of the carbon footprint reduction (\$/kg CO₂e)
4-Bus	7,885	7,816	8,395	80	60,000	7.15
18-Bus	74,578	72,613	239,075	1040	780,000	3.26

Table 15. Economic and Environmental Evaluation

The results above presented reveal the potential of escalation: developing the same strategy of installation in a larger network yields exceptional relative results by reducing the marginal cost more than 50%. In terms of emissions reduction, the enhancement provided for the 18-bus case of 239 tons CO₂e corresponds to nearly 2.7% of the annual emissions of the grid.

However, the nominal value of that cost is still very high and could not be compensated with only a carbon tax. The current value of carbon tax in the countries where it has been implemented varies between \$10-30\$/ton [20]. For the 18-bus case, this translates into maximum savings of around \$7,200 annually, which corresponds to roughly 1% of the required annual investment.

6. Conclusions

This section aims to analyze the implications of the research project carried out in this study. The conclusions are drawn from two different perspectives: methodology and results. Moreover, recommendations are suggested for the future enhancement of the proposed method.

6.1. Methodology

Regarding the methodology proposed in this study, the main aspect worth discussing is the performance of the second part of the research: the control section. The proposed model is a regression model that considers the local measurements in each of the buses in order to predict the optimal dispatch of the batteries. The analysis of the coefficients of the models suggested they could be accepted under a minimum level of significance. On the other hand, the residuals analysis suggested the model was not good enough and that it should be replaced by a different one. However, the conclusions derived from this analysis were discarded because of the size of the sample, and the controls were tested with a simulation of a 2-day operation period of the grid. In order to enhance the performance of this section of the methodology, it could be reasonable to increase the size of the sample by simulating more possible scenarios of the grid during the first step of the study. This way, the decision to discard the proposed regression model could be made based on the residuals analysis.

6.2. Results

From the results perspective, two different assessments are to be made. First, the results yielded by the simulation of the controls suggests it could be worth researching other techniques in order to represent more accurately the behavior of the grid, as well as increasing the size of the sample employed. On the other hand, the reduction in emissions provided by the centralized OPF shows the potential of BESS to reduce the carbon footprint. Harnessing the variation of the grid's carbon intensity throughout the day could lead to substantial reductions in CO₂ emissions without needing to change the present energy mix. Although the cost of implementation of such techniques is high, they could

be harnessed as complementary measures in order to achieve sustainability in the power grid.

6.3. Future Work and Recommendations

This study intended to be an initial step to gain knowledge in the subject and serve as a first step of deeper research. Therefore, several enhancements could be added in the future.

First, as it has already been mentioned, it is necessary to broaden the database used for the design of the controls by simulating more possible operating scenarios of the grid. This way, the obtained model could be more robust and could represent the actual behavior more accurately.

Second, it has been stated throughout the paper that the BESS and the PVs have the potential to inject and draw reactive power from the grid. In future works, it could be worth evaluating how this additional applications could be combined with the use proposed in this study.

Last, the main challenge of implementing these technologies in real price could be their price. It has been stated that a carbon tax is not enough to compensate the cost of the investment; thus, the way to achieve economic viability would be to reduce the price of the batteries, which needs investment in order to enhance the technology. Therefore, staying updated to the developments in the energy storage systems sector is key in order to find a more economical alternative that provides balance between economic and environmental costs.

7. References

- [1] United Nations, (2015), *Paris Agreement*, Available online at: <https://unfccc.int/process-and-meetings/the-paris-agreement/the-paris-agreement/nationally-determined-contributions-ndcs>
- [2] NASA, (2020), *Global Land-Ocean Temperature Index*, Available online at: <https://climate.nasa.gov/vital-signs/global-temperature/>
- [3] Robiou du Pont, Y., (2017), *The Paris Agreement Global Goals: What does a fair share for G20 countries look like?*, Melbourne, The University of Melbourne
- [4] Ritchie, H., (2017), *Renewable Energy*. OurWorldInData.org, Available online at: <https://ourworldindata.org/renewable-energy>
- [5] Alea Soft Energy Forecasting, (2020), *The wind energy caused negative prices in Germany and will lower the markets prices this week*, Available online at: <https://aleasoft.com/wind-energy-caused-negative-prices-germany-lower-european-electricity-markets-prices-this-week/>
- [6] Karagiannopoulos, S. et al, (2019), *Data-driven Local Control Design for Active Distribution Grids using off-line Optimal Power Flow and Machine Learning Techniques*, IEEE
- [7] EEEGuide.com, (2016), *Automatic Voltage Control*, Available online at: <https://www.eeeguide.com/automatic-voltage-control/>
- [8] Csanyi, E., (2015), *4 Essential Features of On-Load Tap Changer (OLTC)*, Electrical Engineering Portal, Available online at: <https://electrical-engineering-portal.com/4-essential-features-of-transformer-on-load-tap-changer-oltc>
- [9] Moshari, A., (2010), *Demand-side behavior in the smart grid environment*, IEEE PES Innovative Smart Grid Technologies Conference, Europe
- [10] Xu, H., (2019), *Data-driven Coordination of Distributed Energy Resources for Active Power Provision*, IEEE Transactions on Power Systems
- [11] ECE 5984: Power Distribution System Analysis, *Lecture 12: Distflow and LinDistFlow*, Blacksburg, Virginia Tech

- [12] EnergySage, (2019), *How to choose the best battery for a solar energy system*, Available online at: <https://www.energysage.com/solar/solar-energy-storage/what-are-the-best-batteries-for-solar-panels/>
- [13] Spyder Developers. (2018) Spyder. Available online at: <https://www.spyder-ide.org/>
- [14] I. Gurobi Optimization, “*Gurobi optimizer reference manual 2019*”. Available online at: <http://www.gurobi.com>
- [15] Zimmerman, R. D., Murillo-Sánchez C. E., and Thomas R. J., *Matpower: Steady-State Operations, Planning and Analysis Tools for Power Systems Research and Education*, Power Systems, IEEE Transactions on, vol. 26, no. 1, pp. 12{19, Feb. 2011. doi: 10.1109/TPWRS.2010.2051168
- [16] Sheng, W. et al, *A Fast Reactive Power Optimization in Distribution Network Based on Large Random Matrix Theory and Data Analysis*”, Applied Sciences, vol. 6, no. 6
- [17] Adrase, (2020), *Datos de Radiación Solar en España*, Available online at: <http://www.adrase.com/acceso-a-los-mapas.html>
- [18] Tomorrow, (2020), *Electricity Map*, built by Tomorrow, Copenhagen, Available online at: <https://www.electricitymap.org/zone/ES>
- [19] MATLAB, (2016). *version 9.10.0(R2016b)*. Natick, Massachusetts: The MathWorks Inc
- [20] Plumer, B. et al, (2019), *These Countries Have Prices on Carbon. Are They Working?*, New York, The New York Times Company

Appendix A: Sustainable Development Goals

The 17 Sustainable Development Goals (SDG) were agreed by the United Nations Members in 2015. The SDGs aim to foster social and economic growth while ensuring the protection of the environment and its resources. Such purpose can be summarized by the following statement: ensure present growth without compromising the prosperity of future generations. For such purpose, the goals defined try to influence all aspects of modern societies, considering the differences in opportunities between developed and developing countries. For instance, objectives such as “Climate Action”, “Protect Life Below Water” and “Protect Life on Land”, are combined with “No Poverty”, “Zero Hunger” and “Decent Work and Economic Growth”. This broad framework provides a wide field of opportunities while setting concrete goals in order to achieve sustainability leaving no one behind.

The main objective of this study is helping to solve one of the main causes of sustainability issues: CO₂ emissions. The emission of this greenhouse effect gas is the consequence of economic and social activities that have enhanced the welfare of humankind. Energy consumption and transportation are two of the sectors that have significantly contributed to the development and growth of modern societies. However, such development has brought a new challenge to societies: how to maintain and further enhance the current standard of life while solving the issues derived from emissions. In such context, renewable energy sources have emerged in order to reduce the CO₂ footprint of the activities of modern society. Its potential to harness natural resources in a responsible way places these new technologies in the main focus of modern scientific research and is continuously mentioned within the framework proposed by the United Nation through the SDGs.

Regarding the connection between this study and the SDGs, it can be inferred from the same objective of this research: this study aims to provide an analysis of the potential to reduce emissions that the installation of Energy Storage Systems could have in a Distribution Network. The initial purpose was to analyze the possibility of benefiting from the variation of the grid’s carbon intensity by storing energy in those devices during low intensity periods and discharging during high intensity periods. The intention was to

increase the effective renewable energy consumed in the grid during a 3-day operation time by scheduling an optimal dispatch of the batteries. Therefore, the primary SDG this study tackles is to “Ensure access to affordable, reliable, sustainable and modern energy for all”, focusing on the target “By 2030, increase substantially the share of renewable energy in the global energy mix” as the primary goal. Moreover, this research addresses sustainability from a consumption point of view, which is summarized in the 12th SDG: “Ensure sustainable consumption and production patterns” with the goal of “By 2030, achieve sustainable management and efficient use of natural resources”. Thus, the proposed methodology provides insight on how the current energy mix could be managed in a more efficient way to enhance its environmental performance.

Being the batteries the main driver of the enhancement discussed in this study, it is worth mentioning that the application studied in this project is not the only one offered by this type of technologies: the ability of batteries to inject and draw reactive power from the grid could really enhance the local control capabilities of distribution networks. However, focusing only on their timely dispatch allows to provide a deeper analysis of their potential to reduce the carbon footprint of the energy consumed. Such analysis is presented in the “Economic and Environmental Impact Assessment” section of this study, providing figures that quantify the monetary costs of the investment. This economic and environmental assessment is summarized in a table in the aforementioned section, which facilitates the understanding of the enhancements achieved and the costs of the implementation of such techniques:

CASE	Emissions without BESS in 3-day period (kg CO₂e)	Emissions with BESS in 3-day period (kg CO₂e)	Annual reduction of emissions (kg CO₂e)	N° of batteries installed	Total annual cost of the batteries (\$)	Marginal cost of the carbon footprint reduction (\$/kg CO₂e)
4-Bus	7,885	7,816	8,395	80	60,000	7.15
18-Bus	74,578	72,613	239,075	1040	780,000	3.26

Table 15 from chapter 5: Economic and Environmental Impact Assessment

The table above presented reveals the enhancements provided by the proposed centralized OPF, which are represented by an annual reduction of 239 tons CO₂e for the 18-bus case. In terms of economic cost, the marginal cost is reduced from the 4-bus case to the 18-bus case by 55%, which suggests the economic performance of the proposed method could be enhanced for larger networks. This results show the potential that batteries could have when used jointly with renewable sources, specifically, with sun power implemented as distributed generation. This coordinated implementation is key in the fulfillment of the SDGs, since it has the potential of providing cheap and clean energy to the consumers while ensuring certain independency from the larger producers. This will be especially important in countries where access to energy is limited and controlled by a minority of the population, which hinders the growth opportunities of the weakest.

To conclude, this study proposes a methodology that enables the reduction of the carbon footprint of a distribution network. Therefore, it is aligned with the SDGs proposed by the United Nations, helping bring ideas to the current standard so that sustainable development can be achieved.

Appendix B: 4-bus Case Data

GRID'S PARAMETERS			
Power Base (MVA)	Voltage Base (KV)	Maximum Voltage (p.u.)	Minimum Voltage (p.u.)
1	12.5	1.1	0.9

BUS DATA				
Bus number	Type of bus	Active Base Load (MW)	Reactive Base Load (Mvar)	Energy Storage Capability (MWh)
1	Slack (V1= 1 p.u.)	-	-	-
2	Demand (commercial)	0.4	0.4	-
3	Demand (industrial)	0.4	0.4	-
4	Generation	0.4	0.4	1.12

GENERATORS DATA		
Bus number	Active Generation Limit (MW)	Reactive Generation Limit (Mvar)
1	-999→999	-999→999
4	0→Solar Availability	No capability

BRANCH DATA			
From bus	To bus	Branch Resistance (p.u.)	Branch Reactance (p.u.)
1	2	0.003	0.006
2	3	0.003	0.006
1	4	0.003	0.006

*Generation nodes are the buses with residential load curves.

Appendix C: 18-bus Case Data

GRID'S PARAMETERS			
Power Base (MVA)	Voltage Base (KV)	Maximum Voltage (p.u.)	Minimum Voltage (p.u.)
1	12.5	1.1	0.9

BUS DATA				
Bus number	Type of bus	Active Base Load (MW)	Reactive Base Load (Mvar)	Energy Storage Capability (MWh)
1	Slack ($V_1 = 1.025$ p.u.)	-	-	-
2	Demand	-	-	-
3	Demand	-	-	-
4	Demand (commercial)	0.2	0.12	-
5	Demand (commercial)	0.4	0.25	-
6	Demand (industrial)	1.5	0.93	-
7	Demand (industrial)	3	2.26	-
8	Generation	0.8	0.5	2.24
9	Generation	0.2	0.12	0.56
10	Generation	1	0.62	2.8
11	Generation	0.5	0.31	1.4
12	Demand (industrial)	1	0.62	-
13	Demand (commercial)	0.3	0.19	-
14	Generation	0.2	0.12	0.56
15	Generation	0.8	0.5	2.24
16	Generation	0.5	0.31	1.4
17	Generation	1	0.62	2.8
18	Generation	0.2	0.12	0.56

GENERATORS DATA		
Bus number	Active Generation Limit (MW)	Reactive Generation Limit (Mvar)
1	-999→999	-999→999
8	0→Solar Availability	No capability
9	0→Solar Availability	No capability
10	0→Solar Availability	No capability
11	0→Solar Availability	No capability
14	0→Solar Availability	No capability
15	0→Solar Availability	No capability
16	0→Solar Availability	No capability
17	0→Solar Availability	No capability
18	0→Solar Availability	No capability

BRANCH DATA			
From bus	To bus	Branch Resistance (p.u.)	Branch Reactance (p.u.)
1	2	0.00004998	0.00035398
2	3	0.000312	0.00675302
3	4	0.00043098	0.00120403
4	5	0.00060102	0.00167699
5	6	0.00031603	0.00088198
6	7	0.000896	0.00250202
7	8	0.00029498	0.000824
8	9	0.00172	0.00212
9	10	0.00407002	0.00305299
4	11	0.00170598	0.00220902

3	12	0.00291002	0.003768
12	13	0.00222202	0.00287699
13	14	0.00480301	0.00621798
13	15	0.00398502	0.00516
15	16	0.00291002	0.003768
15	17	0.00372698	0.00459302
17	18	0.001104	0.00136

*Generation nodes are the buses with residential load curves.

Appendix D: Powerwall Datasheet

POWERWALL

Tesla Powerwall is a fully-integrated AC battery system for residential or light commercial use. Its rechargeable lithium-ion battery pack provides energy storage for solar self-consumption, time-based control, and backup.

Powerwall's electrical interface provides a simple connection to any home or building. Its revolutionary compact design achieves market-leading energy density and is easy to install, enabling owners to quickly realize the benefits of reliable, clean power.



PERFORMANCE SPECIFICATIONS

AC Voltage (Nominal)	120/240 V
Feed-In Type	Split Phase
Grid Frequency	60 Hz
Total Energy	14 kWh
Usable Energy	13.5 kWh
Real Power, max continuous	5 kW (charge and discharge)
Real Power, peak (10 s, off-grid/backup)	7 kW (charge and discharge)
Apparent Power, max continuous	5.8 kVA (charge and discharge)
Apparent Power, peak (10 s, off-grid/backup)	7.2 kVA (charge and discharge)
Maximum Supply Fault Current	10 kA
Maximum Output Fault Current	32 A
Overcurrent Protection Device	30 A
Imbalance for Split-Phase Loads	100%
Power Factor Output Range	+/- 1.0 adjustable
Power Factor Range (full-rated power)	+/- 0.95
Internal Battery DC Voltage	50 V
Round Trip Efficiency ¹	90%
Warranty	10 years

¹Values provided for 20°C (67°F), 3.3 kW charge/discharge power.

²In Backup mode, grid charge power is limited to 3.3 kW.

³AC to battery to AC, at beginning of life.

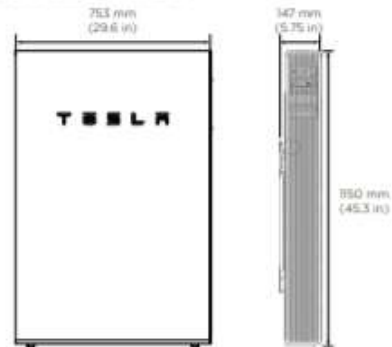
COMPLIANCE INFORMATION

Certifications	UL 9542, UL 1741, UL 1973, UL 9540, IEEE 1547, UN 38.3
Grid Connection	Worldwide Compatibility
Emissions	FCC Part 15 Class B, ICES 003
Environmental	RoHS Directive 2011/65/EU
Seismic	AC156, IEEE 693-2005 (high)

MECHANICAL SPECIFICATIONS

Dimensions ¹	850 mm x 753 mm x 147 mm (45.3 in x 29.6 in x 5.75 in)
Weight ²	84 kg (251.3 lbs)
Mounting options	Floor or wall mount

¹Dimensions and weight differ slightly if manufactured before March 2018. Contact Tesla for additional information.



ENVIRONMENTAL SPECIFICATIONS

Operating Temperature	-20°C to 50°C (-4°F to 122°F)
Recommended Temperature	0°C to 30°C (32°F to 86°F)
Operating Humidity (RH)	Up to 100%, condensing
Storage Conditions	-20°C to 30°C (-4°F to 86°F) Up to 95% RH, non-condensing State of Energy (SoE): 25% initial
Maximum Elevation	3000 m (9843 ft)
Environment	Indoor and outdoor rated
Enclosure Type	NEMA 3R
Ingress Rating	IP67 (Battery & Power Electronics) IP56 (Wiring Compartment)
Wet Location Rating	Yes
Noise Level @ 3m	< 40 dBA at 30°C (86°F)

TESLA

TESLA.COM/ENERGY

Appendix E: 4-bus Grid Centralized OPF Code

The code below presented is the implementation of the centralized OPF for the base case. The 18-bus case code is an expansion and further development of the code here presented. For the complete code: aeo.esteban@gmail.com

```
from gurobipy import *
import math
import openpyxl

def main():
    m=Model("distflow_losses")
    ## Loading of demand profile
    load_file= openpyxl.load_workbook('load_profile.xlsx')
    demand = load_file.get_sheet_by_name('4_bus')
    load_file_2=openpyxl.load_workbook('carbon_intensity_profile.xlsx')
    carbon=load_file_2.get_sheet_by_name('Hoja1')

    m.setParam(GRB.Param.NonConvex, 2)## To solve nonconvex constraints
    m.setParam(GRB.Param.MIPGap,0.0002)

    ## Variables
    # Slack Generation
    pg_1={}
    qg_1={}

    for t in range(1,433):
        pg_1[t]=m.addVar(vtype=GRB.CONTINUOUS, lb=-GRB.INFINITY, ub=GRB.INFINITY,
name="pg_1[%s]"%(t))
        qg_1[t]=m.addVar(vtype=GRB.CONTINUOUS, lb=-GRB.INFINITY, ub=GRB.INFINITY,
name="qg_1[%s]"%(t))

    m.update()

    # PV Generation
    pg_4={}
```

```

for j in range(1,433):

    pg_4[j]=m.addVar(vtype=GRB.CONTINUOUS, lb=0, ub=0.48*demand["D%s"%(j)].value,
name="pg_4[%s]"%(j))

#Injections

pinj={}

qinj={}

for i in 1,2,3,4:

    for z in range(1,433):

        pinj[i,z]=m.addVar(vtype=GRB.CONTINUOUS, lb=-GRB.INFINITY, ub=GRB.INFINITY,
name="pinj[%s,%s]"%(i,z))

        qinj[i,z]=m.addVar(vtype=GRB.CONTINUOUS, lb=-GRB.INFINITY, ub=GRB.INFINITY,
name="qinj[%s,%s]"%(i,z))

    m.update()

#Branch power flow

pbr_14={}

pbr_12={}

pbr_23={}

qbr_14={}

qbr_12={}

qbr_23={}

for u in range(1,433):

    pbr_14[u]=m.addVar(vtype=GRB.CONTINUOUS, lb=-GRB.INFINITY, ub=GRB.INFINITY,
name="pbr_14[%s]"%(u))

    qbr_14[u]=m.addVar(vtype=GRB.CONTINUOUS, lb=-GRB.INFINITY, ub=GRB.INFINITY,
name="qbr_14[%s]"%(u))

    pbr_12[u]=m.addVar(vtype=GRB.CONTINUOUS, lb=-GRB.INFINITY, ub=GRB.INFINITY,
name="pbr_12[%s]"%(u))

    qbr_12[u]=m.addVar(vtype=GRB.CONTINUOUS, lb=-GRB.INFINITY, ub=GRB.INFINITY,
name="qbr_12[%s]"%(u))

```

```

    pbr_23[u]=m.addVar(vtype=GRB.CONTINUOUS, lb=-GRB.INFINITY, ub=GRB.INFINITY,
name="pbr_23[%s]"%(u))

    qbr_23[u]=m.addVar(vtype=GRB.CONTINUOUS, lb=-GRB.INFINITY, ub=GRB.INFINITY,
name="qbr_23[%s]"%(u))

m.update()

#Branch currents
l_14={}
l_12={}
l_23={}
l_45={}

for p in range(1,433):
    l_14[p]=m.addVar(vtype=GRB.CONTINUOUS, lb=0.0, ub=8, name="l_14[%s]"%(p))
    l_12[p]=m.addVar(vtype=GRB.CONTINUOUS, lb=0.0, ub=8, name="l_12[%s]"%(p))
    l_23[p]=m.addVar(vtype=GRB.CONTINUOUS, lb=0.0, ub=8, name="l_23[%s]"%(p))

m.update()

#Bus voltages
v_4={}
v_2={}
v_3={}

for v in range(1,433):
    v_4[v]=m.addVar(vtype=GRB.CONTINUOUS, lb=0.8836, ub=1.21, name="v_4[%s]"%(v))
    v_2[v]=m.addVar(vtype=GRB.CONTINUOUS, lb=0.8836, ub=1.21, name="v_2[%s]"%(v))
    v_3[v]=m.addVar(vtype=GRB.CONTINUOUS, lb=0.8836, ub=1.21, name="v_3[%s]"%(v))

m.update()

#Battery
Pgch={}
Psch={}
Pdis={}

```

```

Ebat={}
xg_ch={}
x_dis={}
xs_ch={}

for h in range(1,433):
    Pgch[h]=m.addVar(vtype=GRB.CONTINUOUS, lb=0, ub=0.56, name="Pgch[%s]"%(h))
    Psch[h]=m.addVar(vtype=GRB.CONTINUOUS, lb=0, ub=0.56, name="Psch[%s]"%(h))
    Pdis[h]=m.addVar(vtype=GRB.CONTINUOUS, lb=0, ub=0.56, name="Pdis[%s]"%(h))
    Ebat[h]=m.addVar(vtype=GRB.CONTINUOUS, lb=0.0432, ub=1.08, name="Ebat[%s]"%(h))
    xg_ch[h]=m.addVar(vtype=GRB.BINARY, name="xg_ch[%s]"%(h))
    x_dis[h]=m.addVar(vtype=GRB.BINARY, name="x_dis[%s]"%(h))
    xs_ch[h]=m.addVar(vtype=GRB.BINARY, name="xs_ch[%s]"%(h))

m.update()

Ebat[0]=m.addVar(vtype=GRB.CONTINUOUS, lb=0.0432, ub=1.08, name="Ebat[0]")

## Objective
OBJ = LinExpr()

for o in range(1,433):
    OBJ = OBJ + pg_1[o]*24/144*carbon["B%s"%o].value

m.setObjective(OBJ, GRB.MINIMIZE)

## Constraints

for h in range(1,433):
    #Injections
    m.addConstr(pinj[1,h]==pg_1[h])
    m.addConstr(pinj[2,h]==-0.4*demand["A%s"%h].value)
    m.addConstr(pinj[3,h]==-0.4*demand["B%s"%h].value)
    m.addConstr(pinj[4,h]==pg_2[h]-0.4*demand["C%s"%h].value-
xg_ch[h]*Pgch[h]+x_dis[h]*Pdis[h])
    m.addConstr(qinj[1,h]==qg_1[h])

```

```

m.addConstr(qinj[2,h]==-0.2*demand["A%s"%h].value)
m.addConstr(qinj[3,h]==-0.2*demand["B%s"%h].value)
m.addConstr(qinj[4,h]==-0.2*demand["C%s"%h].value)
# Battery
m.addConstr(Ebat[0]==0.0432)
m.addConstr(Ebat[h]==Ebat[h-1]+(0.9*Pgch[h]*xg_ch[h]-x_dis[h]*Pdis[h]*1/0.9)*24/144)
m.addConstr(xg_ch[h]+x_dis[h]<=1)
m.addConstr(Ebat[432]==0.0432)
# Bus 1
m.addConstr(pbr_14[h]+pbr_12[h]==pinj[1,h])
m.addConstr(qbr_14[h]+qbr_12[h]==qinj[1,h])
# Bus 4
m.addConstr(0==pbr_14[h]+pinj[4,h]-0.003*I_14[h])
m.addConstr(0==qbr_14[h]+qinj[4,h]-0.006*I_14[h])
# Bus 2
m.addConstr(pbr_23[h]==pinj[2,h]+pbr_12[h]-0.003*I_12[h])
m.addConstr(qbr_23[h]==qinj[2,h]+qbr_12[h]-0.006*I_12[h])
# Bus 3
m.addConstr(0==pbr_23[h]+pinj[3,h]-0.003*I_23[h])
m.addConstr(0==qbr_23[h]+qinj[3,h]-0.006*I_23[h])

#Current constraints
m.addConstr(l_12[h]==pbr_12[h]*pbr_12[h] + qbr_12[h]*qbr_12[h])
m.addConstr(l_14[h]==pbr_14[h]*pbr_14[h] + qbr_14[h]*qbr_14[h])
m.addConstr(l_23[h]*v_2[h]==pbr_23[h]*pbr_23[h] + qbr_23[h]*qbr_23[h])

##Voltages
m.addConstr(v_4[h]== 1 - 2*0.003*pbr_14[h] - 2*0.006*qbr_14[h] + (pow(0.003,2) +
pow(0.006,2))*I_14[h])

```

```

    m.addConstr(v_2[h]== 1 - 2*0.003*pbr_12[h] - 2*0.006*qbr_12[h] + (pow(0.003,2) +
pow(0.006,2))*l_12[h])

    m.addConstr(v_3[h]== v_2[h] - 2*0.003*pbr_23[h] - 2*0.006*qbr_23[h] + (pow(0.003,2) +
pow(0.006,2))*l_23[h])

m.optimize();

opt_soln = {}
for xx in m.getVars():
    opt_soln[xx.varName] = xx.x

print '-----'

for i in range(1,433):

    print",opt_soln['v_2[%s]%(i)],opt_soln['v_3[%s]%(i)],opt_soln['v_4[%s]%(i)],
opt_soln['pg_1[%s]%(i)],opt_soln['pg_4[%s]%(i)],opt_soln['qg_1[%s]%(i)],opt_soln['l_12[%s]'
%(i)],opt_soln['l_23[%s]%(i)],opt_soln['l_14[%s]%(i)],opt_soln['Pgch[%s]%(i)],opt_soln['Pdis[
%s]%(i)],opt_soln['Ebat[%s]%(i)]

    print 'obj_primal=',m.objval

main();

```

Appendix F: 18-bus Grid Local Control Simulation Code

The code below presented is just a sample of the complete simulation code. It represents the description of the behavior of bus 15 following the steps described in the control test section. For the complete code: aeo.esteban@gmail.com

```
%Bus 15: prediction
bat_pred_15(i+1,1)=feval(model_15, demand_active_var(i+1,15),
pg15(i+1,1), dod_15(i+1,1), pg15_2(i+1,1), v15_2(i,1));

discharge_limit_15=96.43-dod_15(i+1,1);
charge_limit_15=dod_15(i+1,1);
bat_comm_15(i+1,1)=bat_pred_15(i+1,1);
    if (bat_pred_15(i+1,1)>=0)
        a=bat_pred_15(i+1,1)*(24/144)*100/(0.9*2.24);
        if (a>=discharge_limit_15)
            if
(discharge_limit_15>=(power_spec_15*24/(0.9*144)*100/2.24))
                bat_pred_15(i+1,1)=power_spec_15;
            else
bat_pred_15(i+1,1)=discharge_limit_15*2.24/100*0.9*144/24;
            end
        else
            if (a>=(power_spec_15*24/(0.9*144)*100/2.24))
                bat_pred_15(i+1,1)=power_spec_15;
            else
                bat_pred_15(i+1,1)=bat_pred_15(i+1,1);
            end
        end
    end
    %Update battery energy
    ebat_15(i+1,1)=ebat_15(i,1)-bat_pred_15(i+1,1)/0.9*24/144;
else
    a=-bat_pred_15(i+1,1)*(24/144)*0.9*100/2.24;
    if (a>=charge_limit_15)
        if
(charge_limit_15>=(power_spec_15*24*0.9/144*100/2.24))
            bat_pred_15(i+1,1)=-power_spec_15;
        else
bat_pred_15(i+1,1)=charge_limit_15*2.24/100/0.9*144/24;
        end
    else
        if (a>=(power_spec_15*24*0.9/144*100/2.24))
            bat_pred_15(i+1,1)=-power_spec_15;
        else
            bat_pred_15(i+1,1)=bat_pred_15(i+1,1);
        end
    end
end
```



```

    %Update battery energy
    ebat_15(i+1,1)=ebat_15(i,1)-bat_pred_15(i+1,1)*0.9*24/144;
end
    %Update charging and discharging limits
discharge_limit_15=(ebat_15(i+1,1)-0.0357*2.24)*100/2.24;
charge_limit_15=(2.24-ebat_15(i+1,1))*100/2.24;
dod_15(i+2,1)=charge_limit_15;


---


%Update Injections, when positive as demands, when negative as
generations

%Bus 15
    if (bat_pred_15(i+1,1)>=0)
        mpc.gen(15, PG)=bat_pred_15(i+1,1)+pg15(i+1,1);
        mpc.bus(15, PD)=demand_active_var(i+1,15);

    else
        mpc.gen(15, PG)=pg15(i+1,1);
        mpc.bus(15, PD)=demand_active_var(i+1,15)-
bat_pred_15(i+1,1);

    end



---


%Run Power Flow and Obtain Voltages
[v,p,q]=distflow_lossy(mpc);
v15(i+1,1)=v(15,1);
v15_2(i+1,1)=v(15,1)^2;


---


%Update demands and run power flow again

```